IEEE Access
Multidisciplinary | Rapid Review | Open Access Journal

Received November 1, 2019, accepted November 16, 2019, date of publication November 22, 2019,
date of current version December 5, 2019.

Digital Object Identifier 10.1109/ACCESS.2019.2955118

Performance Analysis of Buffer-Aided Hybrid NOMA/OMA in Cooperative Uplink System

PENG XU[1], (Member, IEEE), JIANPING QUAN[1], ZHENG YANG[2], (Member, IEEE), GAOJIE CHEN[3], (Senior Member, IEEE), AND ZHIGUO DING[4], (Member, IEEE)

[1]Chongqing Key Laboratory of Mobile Communications Technology, School of Communication and Information Engineering, Chongqing University of Posts and Telecommunications, Chongqing 400065, China
[2]Fujian Provincial Engineering Technology Research Center of Photoelectric Sensing Application, Key Laboratory of OptoElectronic Science and Technology for Medicine of Ministry of Education, Fujian Normal University, Fuzhou 350007, China
[3]School of Engineering, University of Leicester, Leicester LE1 7RH, U.K.
[4]School of Electrical and Electronic Engineering, The University of Manchester, Manchester M13 9PL, U.K.

Corresponding author: Zheng Yang (zyfjnu@163.com)

The work of P. Xu and J. Quan was supported in part by the National Natural Science Foundation of China under Grant 61701066, in part by the Chongqing Natural Science Foundation Project under Grant cstc2019jcyj-msxm1354, in part by the Chongqing College Students' Innovative Entrepreneurial Training Plan Program under Grant S201910617032, and in part by the Special Funded Undergraduate Research Training Program under Grant A2019-39. The work of Z. Yang was supported in part by the National Natural Science Foundation of China under Grant 61701118, Grant U1805262, Grant 61871131, and Grant 61901117, and in part by the Natural Science Foundation of Fujian Province, China, under Grant 2018J05101 and Grant 2019J01267. The work of G. Chen was supported by the EPSRC funding under Grant EP/R006377/1 (M3NETs). The work of Z. Ding was supported in part by the UK EPSRC under Grant EP/P009719/2, and in part by the H2020-MSCA-RISE-2015 under Grant 690750.

ABSTRACT This paper investigates a cooperative uplink system where two users wish to send messages to a base station with the help of a buffer-aided relay. Transmission modes in terms of both non-orthogonal multiple access (NOMA) and orthogonal multiple access (OMA) are considered. For the considered system, the probability for the user-to-relay channels to successfully perform NOMA is first theoretically derived in two scenarios of dynamic and fixed power controls (PCs) at users. Then, an efficient buffer-aided hybrid NOMA/OMA based mode selection (MS) scheme is proposed, which adaptively switches between the NOMA and OMA transmission modes according to the instantaneous strength of wireless channels and the buffer state. The state transmission matrix probabilities of the corresponding Markov chain is also derived, and the performance of the proposed hybrid NOMA/OMA scheme is analyzed with closed-form expressions, in terms of sum throughput, outage probability, diversity gain, and average packet delay. For both the dynamic and fixed PCs, the proposed scheme is proved to achieve a diversity gain of two when the buffer size is not smaller than three, which means that fixed PC will not lead to a loss of diversity gain.

INDEX TERMS NOMA, hybrid NOMA/OMA, buffer-aided relay, mode selection, power control.

I. INTRODUCTION

Non-orthogonal multiple access (NOMA) technology, using successive interference cancellation (SIC) and multiplexing in power-domain, can improve spectrum efficiency, which is considered to be a promising fifth-generation mobile communication technology [1]. NOMA allows multiple users to share the communication resources simultaneously, i.e., time, frequency and code domain, then achieves better performance than conventional orthogonal multiple access (OMA) [2]–[4].

The associate editor coordinating the review of this manuscript and approving it for publication was Lei Guo.

Cooperative communication can further enhance the efficiency and reliability, and expand the coverage of wireless communication networks. In order to enhance the performance of NOMA, the work in [5] first exploited cooperation between the users, i.e., the stronger users help the other weaker users by using the decode-and-forward (DF) scheme, so that the optimal diversity gain can be achieved. On the other hand, the work in [6], [7] investigated cooperative NOMA with a single relay, where multiple users were helped by a dedicated relay node using the DF and amplify-and-forward (AF) schemes. In addition, relay selection (RS) scheme has also been proposed for cooperative NOMA networks with multiple relays in some existing works

(e.g., [8]–[11]). Recently, the uplink cooperative communication has also been investigated in [12], where a coordinated direct and relay transmission was proposed.

Buffer-aided cooperative communication technique can provide additional freedom for wireless cooperative communication networks, which overcomes the bottleneck effect of conventional cooperative communication technologies [13]. Exiting works related to buffer-aided cooperative communication mainly considered the design of adaptive link or mode selection (MS) schemes for single-relay systems (e.g., [14]–[19]), and the design of relay selection schemes for multiple-relay systems [20]–[22]. In addition, buffer-aided cooperative NOMA for downlink transmission has also been investigated in recent existing works [23]–[26]. The works in [23] and [24] considered cooperative NOMA with a single buffer-aided relay. In [23], adaptive and fixed rates were assumed for the source-to-relay and relay-to-user transmissions, respectively, and the sum throughput was maximized based on the optimal MS scheme. In [24], fixed rate was assumed for both the source-to-relay and relay-to-user transmissions, and a relay decision scheme was proposed to enhance outage performance, under the assumptions of fixed and adaptive power allocations at the relay, respectively. Recently, the works in [27], [28] proposed hybrid buffer-aided NOMA/OMA RS scheme for downlink systems, which is shown to significantly outperform NOMA and OMA RS schemes.

Unlike the widely considered downlink buffer-aided relay systems [23]–[28], this paper investigates an uplink buffer-aided relay system with two users, a DF relay, and a base station (BS), where both the modes of NOMA and OMA are considered for the user-to-relay transmission. Note that performance analysis regarding to uplink NOMA is more complicated than that of the downlink NOMA, in the sense that the receiver for uplink NOMA is involved with multiple links from multiple transmitters, whereas each receiver for downlink NOMA is involved with only one link from the single transmitter. The main contributions are summarized as follows:

- We theoretically derive the probability for the user-to-relay channels to successfully perform NOMA in two scenarios of dynamic and fixed power controls (PCs) at users. In particular, for both dynamic and fixed PCs, we carefully designed the transmit power at each user so that the power of the inter-user interference can be controlled.
- We propose an efficient buffer-aided hybrid NOMA/OMA based MS scheme, which adaptively switches between the NOMA and OMA transmission modes according to the instantaneous channel state information (CSI) and the buffer state. The basic idea of the proposed hybrid NOMA/OMA MS scheme is to give priority to the NOMA transmission mode, i.e., NOMA will be adopted to transmit the two users' messages simultaneously. However, the NOMA transmission mode might not be successful, especially for weak channel conditions; in this case, the transmission mode will switch to the OMA.
- The Markov chain (MC) of the proposed hybrid NOMA/OMA based MS scheme is formulated, and the corresponding state transmission probabilities are analyzed. Accordingly, the performance of the proposed hybrid NOMA/OMA MS scheme is derived with closed-form expressions for sum throughput, outage probability, and average packet delay.
- It is demonstrated that the proposed scheme can achieve a diversity gain of two as long as the buffer size is not smaller than three, for both two scenarios of dynamic and fixed PCs. This means that fixed PC will not lead to a loss of diversity gain, by carefully designing the transmit power at each user.

This paper is organized as follows. In Section II, the system model and five transmission modes including CSI and buffer requirements are introduced. Section III derives the probability for the user-to-relay channels to successfully perform NOMA in two scenarios of dynamic and fixed PCs at users. Then Section IV describes the proposed hybrid NOMA/OMA MS scheme. In Section V, the throughput, outage probability, diversity gain, and average packet delay are derived. Section VI provides numerical results to compare the performance of hybrid NOMA/OMA with conventional NOMA and OMA. We conclude this paper in Section VII.

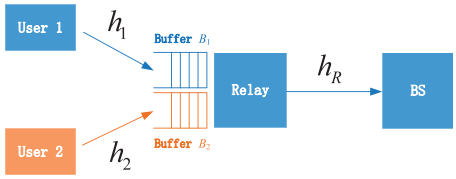

FIGURE 1. System Model of an uplink buffer-aided relaying system.

II. SYSTEM MODEL AND PRELIMINARIES

A. SYSTEM MODEL

Consider a buffer-aided uplink DF relaying system which consists of two users, a relay, and a BS, as shown in Fig. 1. We assume that the direct links between the two users and the BS are not available since they are blocked due to long-distance path loss or obstacles, and the user-relay and relay-BS channels experience identical and independent Rayleigh fading [20]. It is assumed that the time duration is partitioned into slots with equal length and each transmitted packet spans one time slot. In each time slot, the users or the relay may be selected to transmit packets. When each user is selected, it assembles an information symbol intended for the BS into a packet with r_0 bits, i.e., the same target rate of $r_0/2$ BPCU is assumed for each user to guarantee fairness [24], and hence the target sum rate rate is r_0 BPCU. The relay is equipped with two buffers, i.e., B_1 and B_2. Each buffer consists of $L \geq 2$ storage units and each storage unit can store a data packet

TABLE 1. Necessary requirements for each Transmission Mode (T: Transmit; R: Receive; S: Silent), where π_1 and π_2 denotes the descending order of the channel gains so that $H_{\pi_1} \geq H_{\pi_2}$.

Mode	User 1	User 2	Relay	BS	CSI Requirement	Buffer Requirement
$\mathcal{M}_1$	T	S	R	S	$\mathcal{R}_1 \triangleq \bigcup_{H_1}\{H_1 \geq \epsilon_0\}$	$l_1 < L$
$\mathcal{M}_2$	S	T	R	S	$\mathcal{R}_2 \triangleq \bigcup_{H_2}\{H_2 \geq \epsilon_0\}$	$l_2 < L$
$\mathcal{M}_3$	T	T	R	S	$\mathcal{R}_3 \triangleq \bigcup_{(H_1,H_2)}\left\{\begin{array}{l}\frac{H_{\pi_1}P_{\pi_1}}{\sigma^2+H_{\pi_2}P_{\pi_2}} \geq \rho\epsilon_0 \\ H_{\pi_2}P_{\pi_2} \geq P\epsilon_0\end{array}\right\}$	$\max\{l_1, l_2\} < L$
$\mathcal{M}_4$	S	S	T	R	$\mathcal{R}_4 \triangleq \bigcup_{H_R}\{H_R \geq \epsilon_R\}$	$\min\{l_1, l_2\} > 0$
$\mathcal{M}_5$	S	S	S	S	$\forall H_1, H_2, H_R$	$\forall l_1, l_2$

received from any user. A storage unit at buffer B_u is used to store an information symbol transmitted by user u, $u = 1, 2$. If the relay is selected, it retrieves information symbols from the buffers and transmits them to the BS. Assume that each user always has information symbols to transmit.

The channel coefficients from user u to the relay and from the relay to the BS are denoted as h_u and h_R, respectively. Each channel is modeled as $h_i = d_i^{-\gamma/2} g_i$, where the small scale fading gain is Rayleigh distributed, i.e., $g_i \sim \mathcal{CN}(0, 1)$, $i \in \{1, 2, R\}$; thus, we define $H_i \triangleq |h_i|^2$, which follows exponential distributions with means $\Omega_i = d_i^{-2}$. These channels are assumed to be independent flat Rayleigh block fading channels which remain constant during one time slot and change randomly from one time slot to anther. Without loss of generality, it is assumed that each user u and the relay are constrained by the maximum transmit power P, and each receiver has the same noise power σ^2. This implies that individual power constraints at the users are considered in the uplink system, which is more practical than the assumption of the sum power constraint at the users in many existing works for uplink NOMA (e.g., [3], [12]).

For the proposed system, we consider five possible transmission modes, denoted by $\mathcal{M}_1, \cdots, \mathcal{M}_5$. Specifically, $\mathcal{M}_1$, $\mathcal{M}_2$, and $\mathcal{M}_3$ denote the user-to-relay modes, where the opportunistic hybrid NOMA/OMA scheme is utilized: $\mathcal{M}_1$ and $\mathcal{M}_2$ utilize the OMA scheme for which only one of the users is selected to transmit a packet to the relay, and $\mathcal{M}_3$ utilizes the NOMA scheme for which the two users transmit packets to the relay simultaneously. $\mathcal{M}_4$ denotes the relay-to-BS mode, where the relay selects a packet from each user's buffer and blends the two packets into a mixed packet with $2r_0$ bits and then transmits it to the BS[1]; and $\mathcal{M}_5$ denotes the silent mode.

B. TRANSMISSION MODES AND CSI REQUIREMENTS

The instantaneous CSI requirement for each mode is summarized in Table 1, where the CSI region of mode $\mathcal{M}_k$ is defined as $\mathcal{R}_k$. Specifically, for the mode $\mathcal{M}_u$, $u = 1, 2$, it requires $H_u \geq \epsilon_0$ so that the relay can decode packets correctly, where $\epsilon_0 \triangleq \frac{2^{r_0}-1}{\rho}$, and $\rho \triangleq \frac{P}{\sigma^2}$ denote the maximum transmit SNR for each node. For the mode $\mathcal{M}_4$, the transmission rate from the relay to the BS should be $2r_0$ bits per channel use (BPCU), so $H_R \geq \epsilon_R$ is required, where $\epsilon_R \triangleq \frac{2^{2r_0}-1}{\rho}$. For the uplink NOMA mode $\mathcal{M}_3$, the relay receives the following signal:

$$y_R = h_1\sqrt{P_1}x_1 + h_2\sqrt{P_2}x_2 + n_r, \tag{1}$$

where $P_u \leq P$ is the transmit power at user u, $u = 1, 2$, and n_r is the additive Gaussian noise at the relay with zero mean and variance σ^2. The relay uses successive interference cancellation (SIC)[2] to decode the two users' messages. It may also be interesting to combine uplink NOMA with some emerging advanced techniques (e.g., mobile edge computing [30], automatic modulation classification [31] and deep leaning [32], [33]), which is out the scope of this paper. Specifically, we assume that the users are sorted according to their channel qualities and denote (π_1, π_2) as the *descending order* of the channel gains, i.e., $|h_{\pi_1}| \geq |h_{\pi_2}|$, where $(\pi_1, \pi_2) = (1, 2)$, if $|h_1| \geq |h_2|$, and $(\pi_1, \pi_2) = (2, 1)$, otherwise. The relay first decodes the message of the stronger user π_1 by treating the weaker user's signal as pure noise, which requires $\frac{H_{\pi_1}P_{\pi_1}}{\sigma^2+H_{\pi_2}P_{\pi_2}} \geq \rho\epsilon_0$; then, it cancels the signal of the stronger user π_1 from the observed signal, $H_{\pi_2}P_{\pi_2} \geq P\epsilon_0$.

Remark 1: Since SIC at the relay first decodes the stronger user's messages, the optimal choice of the transmit power P_{π_1} at the stronger user obviously is P, so we set $P_{\pi_1} = P$. However, the transmit power P_{π_2} at the weaker user should be controlled to be a suitable value, since a larger P_{π_2} will lead to a larger inter-user interference power when using SIC to decode the stronger user's messages at the relay. In the next section, both the dynamic and fixed PCs at the users will be considered, which correspond to two scenarios that the weaker user knows perfect CSI and statistical CSI, respectively.

C. THE BUFFER REQUIREMENTS

Let l_u denote the number of packets in buffer B_u at the end of each time slot, $l_u \in \{0, 1, \ldots, L\}$. The buffer requirement for each mode is also summarized in Table 1, where mode $\mathcal{M}_u$ requires that buffer B_u is not full, i.e., $l_u < L$, $u = 1, 2$;

[1]Note that, different to the user-to-relay transmission, we consider only one mode for the relay-to-BS transmission (i.e. $\mathcal{M}_4$), where the relay transmits both the two users' messages simultaneously, such that the two users' messages can reach the BS at the same time slot and short-term user fairness can be guaranteed [4], [9], [24].

[2]Compared to "joint decoding" [29], SIC enjoys much lower decoding complexity, and hence this paper adopts the SIC detection at the relay.

mode $\mathcal{M}_3$ requires that both the two buffers are not full, i.e., $\max\{l_1, l_2\} < L$; and mode $\mathcal{M}_4$ requires that both the two buffers are not empty, i.e., $\min\{l_1, l_2\} > 0$.

III. PROBABILITY FOR USER-TO-RELAY CHANNELS TO PERFORM NOMA

In this section, we will derive the probability for the user-to-relay channels to successfully perform NOMA, denoted by $P_{\mathcal{R}_3} \triangleq \mathbb{P}\{(H_1, H_2) \in \mathcal{R}_3\}$, in the scenarios of dynamic and fixed PCs at the weaker user, respectively. With the setting of $P_{\pi_1} = P$, we first rewrite the region of $\mathcal{R}_3$ regarding to the NOMA mode $\mathcal{M}_3$, shown in Table 1, as follows:

$$\mathcal{R}_3 = \bigcup_{(H_1,H_2)} \left\{ \begin{array}{l} \dfrac{H_{\pi_1}}{\sigma^2 + H_{\pi_2} P_{\pi_2}} \geq \dfrac{\epsilon_0}{\sigma^2} \\ H_{\pi_2} P_{\pi_2} \geq P\epsilon_0 \end{array} \right\}, \tag{2}$$

where $H_{\pi_1} \geq H_{\pi_2}$. Now, we will design the transmit power at the weaker user to control the power of the inter-user interference in two scenarios of dynamic and fixed PCs in the following two subsections, respectively.

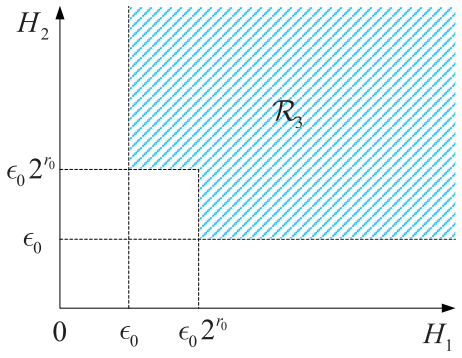

FIGURE 2. Illustration of the region $\mathcal{R}_3$ with dynamic PC.

A. DYNAMIC POWER CONTROL

Dynamic PC corresponds to the scenario that the weaker user knows the perfect CSI of H_{π_2} at the beginning of each time shot, where the perfect CSI can be obtained based on pilot symbols transmitted from the relay to the weaker user. In this case, the weaker user dynamically adjusts its transmit power according to instantaneous CSI, such that the stronger user can be affected minimally by the interference generated by the weaker user in the decoding process at the relay. Specifically, for user π_2, we set the minimum required transmit power, i.e., $P_{\pi_2} \triangleq \frac{P\epsilon_0}{H_{\pi_2}}$ if $\frac{\epsilon_0}{H_{\pi_2}} \leq 1$, and $P_{\pi_2} \triangleq 0$, otherwise, in order to control the power of the inter-user interference when decoding user π_1's messages. Using this power setting, the required CSI region $\mathcal{R}_3$ in (2) can be simplified as follows:

$$\mathcal{R}_3 \triangleq \bigcup_{(H_1,H_2)} \left\{ \begin{array}{l} H_{\pi_1} \geq \epsilon_0 2^{r_0} \\ H_{\pi_2} \geq \epsilon_0 \end{array} \right\}. \tag{3}$$

Fig. 2 illustrates the region $\mathcal{R}_3$ in (3). Thus, we can derive the probability $P_{\mathcal{R}_3}$ as follows:

$$\begin{aligned} P_{\mathcal{R}_3} &= \int_{\epsilon_0}^{+\infty} \int_{\epsilon_0}^{+\infty} \left(\frac{1}{\Omega_1} e^{-\frac{x}{\Omega_1}}\right)\left(\frac{1}{\Omega_2} e^{-\frac{y}{\Omega_2}}\right) \mathrm{d}x\mathrm{d}y \\ &\quad - \int_{\epsilon_0}^{\epsilon_0 2^{r_0}} \int_{\epsilon_0}^{\epsilon_0 2^{r_0}} \left(\frac{1}{\Omega_1} e^{-\frac{x}{\Omega_1}}\right)\left(\frac{1}{\Omega_2} e^{-\frac{y}{\Omega_2}}\right) \mathrm{d}x\mathrm{d}y \\ &= e^{-\epsilon_0\left(\frac{2^{r_0}}{\Omega_1} + \frac{1}{\Omega_2}\right)} + e^{-\epsilon_0\left(\frac{2^{r_0}}{\Omega_2} + \frac{1}{\Omega_1}\right)} - e^{-\left(\frac{1}{\Omega_1} + \frac{1}{\Omega_2}\right)\epsilon_0 2^{r_0}}. \end{aligned} \tag{4}$$

B. FIXED POWER CONTROL

Fixed PC corresponds to the scenario that the weaker user only knows the statistical CSI (i.e., means and variances of fading channels) rather than the perfect CSI of H_{π_2}. In this case, the weaker user π_2 can only adopt a fixed transmit power, which is not larger than P in each time slot. In particular, we set $P_{\pi_2} = \alpha P$, where $0 < \alpha \leq 1$ which is a fixed power parameter to control the transmit power of the weaker user in each time slot. Then we transform the region $\mathcal{R}_3$ in (2) as follows:

$$\mathcal{R}_3 = \bigcup_{(H_1,H_2)} \left\{ \begin{array}{l} H_{\pi_1} \geq \epsilon_0 + H_{\pi_2}\alpha(2^{r_0} - 1) \\ H_{\pi_2} \geq \frac{\epsilon_0}{\alpha} \end{array} \right\}. \tag{5}$$

From (5), one can observe that a larger α is beneficial to decode user π_2's messages but harmful to decode user π_1's messages. To balance the decoding of both the two users' messages, we define the power parameter α as follows:

$$\alpha \triangleq \left\{ \begin{array}{ll} \dfrac{1}{2^{r_0} - 1}, & \text{if } r_0 \geq 1, \\ 1, & \text{if } r_0 < 1. \end{array} \right. \tag{6}$$

Remark 2: α in (6) is naturally designed, whose motivation is to set the coefficient of H_{π_2} in the first term of (5), i.e., $\alpha(2^{r_0} - 1)$, to be 1 if $r_0 \geq 1$, so that the inter-user interference power generated by the weaker user π_2 can be effectively controlled. However, if $r_0 < 1$, the coefficient $\alpha(2^{r_0} - 1)$ cannot exceeds 1 for any $\alpha \in (0, 1]$. In this case, we simply set $\alpha = 1$, as the inter-user interference power can be controlled even if the weaker user π_2 sets its transmit power to be P.

The following proposition gives the expressions for $P_{\mathcal{R}_3}$ in two cases that $r_0 \geq 1$ and $r_0 < 1$.

Proposition 1: Using fixed PC parameter given in (6) at the weaker user, the probability of $P_{\mathcal{R}_3}$ can be expressed in the equation shown at the bottom of the next page.

Proof 1: In the following, we will derive $P_{\mathcal{R}_3}$ by considering two cases that $r_0 \geq 1$ and $r_0 < 1$.

1) CASE I ($R_0 \geq 1$)

Using the definition in (6), the region $\mathcal{R}_3$ in (5) can be expressed as

$$\mathcal{R}_3 = \bigcup_{(H_1,H_2)} \left\{ \begin{array}{l} H_{\pi_1} \geq \epsilon_0 + H_{\pi_2} \\ H_{\pi_2} \geq \epsilon_0(2^{r_0} - 1) \end{array}, \right\} \tag{7}$$

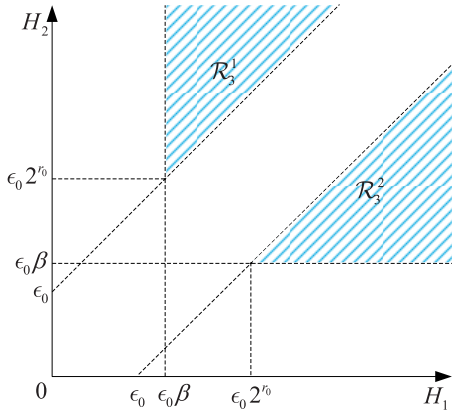

FIGURE 3. Illustration of region $\mathcal{R}_3$ with fixed PC, where $r_0 \geq 1$ and $\beta \triangleq 2^{r_0} - 1$.

which is illustrated in Fig. 3. We observe that $\mathcal{R}_3 = \mathcal{R}_3^1 \bigcup \mathcal{R}_3^2$, where

$$\mathcal{R}_3^1 \triangleq \bigcup_{(H_1,H_2)} \left\{ \begin{matrix} H_1 \geq \epsilon_0 + H_2 \\ H_2 \geq \epsilon_0(2^{r_0}-1) \end{matrix} \right\},$$
$$\mathcal{R}_3^2 \triangleq \bigcup_{(H_1,H_2)} \left\{ \begin{matrix} H_2 \geq \epsilon_0 + H_1 \\ H_1 \geq \epsilon_0(2^{r_0}-1) \end{matrix} \right\}. \quad (8)$$

Now, we first derive $\mathcal{R}_3^1$ as follows:

$$\begin{aligned} P_{\mathcal{R}_3^1} &= \int_{\epsilon_0 2^{r_0}}^{+\infty} \int_{\zeta_1}^{y-\epsilon_0} \left(\frac{1}{\Omega_1} e^{-\frac{x}{\Omega_1}}\right)\left(\frac{1}{\Omega_2} e^{-\frac{y}{\Omega_2}}\right) \mathrm{d}x\mathrm{d}y \\ &= e^{-\frac{1}{\Omega_1}\epsilon_0(2^{r_0}-1)} \int_{\epsilon_0 2^{r_0}}^{+\infty} \frac{1}{\Omega_2} e^{-\frac{y}{\Omega_2}} \mathrm{d}y \\ &\quad - \frac{1}{\Omega_2} e^{\frac{1}{\Omega_1}\epsilon_0} \int_{\epsilon_0 2^{r_0}}^{+\infty} e^{-\left(\frac{y}{\Omega_1}+\frac{y}{\Omega_2}\right)} \mathrm{d}y \\ &= \frac{\Omega_2}{\Omega_1+\Omega_2} e^{-\epsilon_0 2^{r_0}\left(\frac{1}{\Omega_1}+\frac{1}{\Omega_2}\right)+\frac{\epsilon_0}{\Omega_1}}, \end{aligned} \quad (9)$$

where $\zeta_1 = \epsilon_0(2^{r_0}-1)$. Similarly, we have

$$\begin{aligned} P_{\mathcal{R}_3^2} &= \int_{\epsilon_0 2^{r_0}}^{+\infty} \int_{\zeta_1}^{x-\epsilon_0} \left(\frac{1}{\Omega_2} e^{-\frac{y}{\Omega_2}}\right)\left(\frac{1}{\Omega_1} e^{-\frac{x}{\Omega_1}}\right) \mathrm{d}y\mathrm{d}x \\ &= e^{-\frac{1}{\Omega_2}\epsilon_0(2^{r_0}-1)} \int_{\epsilon_0 2^{r_0}}^{+\infty} \frac{1}{\Omega_1} e^{-\frac{x}{\Omega_1}} \mathrm{d}x \\ &\quad - \frac{1}{\Omega_1} e^{\frac{1}{\Omega_2}\epsilon_0} \int_{\epsilon_0 2^{r_0}}^{+\infty} e^{-\left(\frac{x}{\Omega_2}+\frac{x}{\Omega_1}\right)} \mathrm{d}x \\ &= \frac{\Omega_1}{\Omega_1+\Omega_2} e^{-\epsilon_0 2^{r_0}\left(\frac{1}{\Omega_1}+\frac{1}{\Omega_2}\right)+\frac{\epsilon_0}{\Omega_2}}. \end{aligned} \quad (10)$$

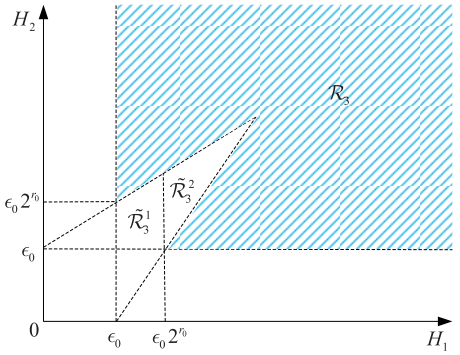

FIGURE 4. Illustration of region $\mathcal{R}_3$ with fixed PC, where $r_0 < 1$.

Combining (9) and (10), we can obtain the expression of $P_{\mathcal{R}_3}$ as shown in (7) for the case $r_0 \geq 1$.

2) CASE II ($R_0 < 1$)

In this case, $P_{\pi_2} = P$ as shown in (6), so the region $\mathcal{R}_3$ in (5) can be expressed as

$$\mathcal{R}_3 = \bigcup_{(H_1,H_2)} \left\{ \begin{matrix} H_{\pi_1} \geq \epsilon_0 + (2^{r_0}-1)H_{\pi_2} \\ H_{\pi_2} \geq \epsilon_0 \end{matrix} \right\}, \quad (11)$$

which is illustrated in Fig. 4. We can observe that $\mathcal{R}_3 \bigcup \tilde{\mathcal{R}}_3^1 \bigcup \tilde{\mathcal{R}}_3^2 = \bigcup_{(H_1,H_2)} \left\{ \begin{matrix} H_1 \geq \epsilon_0 \\ H_2 \geq \epsilon_0 \end{matrix} \right\}$, where

$$\tilde{\mathcal{R}}_3^1 \triangleq \bigcup_{(H_1,H_2)} \left\{ \begin{matrix} \epsilon_0 \leq H_1 \leq \epsilon_0 2^{r_0} \\ \epsilon_0 \leq H_2 \leq \epsilon_0 + (2^{r_0}-1)H_1 \end{matrix} \right\}, \quad (12)$$

$$\tilde{\mathcal{R}}_3^2 \triangleq \bigcup_{(H_1,H_2)} \left\{ \begin{matrix} \epsilon_0 2^{r_0} \leq H_1 \leq \epsilon_0 + (2^{r_0}-1)H_2 \\ H_2 \leq \epsilon_0 + (2^{r_0}-1)H_1 \end{matrix} \right\}. \quad (13)$$

Thus, the probability $P_{\mathcal{R}_3}$ can be expressed as

$$\begin{aligned} P_{\mathcal{R}_3} &= \int_{\epsilon_0}^{+\infty} \int_{\epsilon_0}^{+\infty} \left(\frac{1}{\Omega_1} e^{-\frac{x}{\Omega_1}}\right)\left(\frac{1}{\Omega_2} e^{-\frac{y}{\Omega_2}}\right) \mathrm{d}x\mathrm{d}y - P_{\tilde{\mathcal{R}}_3^1} - P_{\tilde{\mathcal{R}}_3^2} \\ &= e^{-\epsilon_0\left(\frac{1}{\Omega_1}+\frac{1}{\Omega_2}\right)} - P_{\tilde{\mathcal{R}}_3^1} - P_{\tilde{\mathcal{R}}_3^2}. \end{aligned} \quad (14)$$

Now, we first derive $P_{\tilde{\mathcal{R}}_3^1}$ as follows:

$$\begin{aligned} P_{\tilde{\mathcal{R}}_3^1} &= \int_{\epsilon_0}^{\epsilon_0 2^{r_0}} \int_{\epsilon_0}^{\zeta_2} \left(\frac{1}{\Omega_2} e^{-\frac{y}{\Omega_2}}\right)\left(\frac{1}{\Omega_1} e^{-\frac{x}{\Omega_1}}\right) \mathrm{d}y\mathrm{d}x \\ &= \int_{\epsilon_0}^{\epsilon_0 2^{r_0}} \frac{1}{\Omega_1} e^{-\frac{x}{\Omega_1}} \left[e^{-\frac{1}{\Omega_2}\epsilon_0} - e^{-\frac{1}{\Omega_2}((2^{r_0}-1)x+\epsilon_0)} \right] \mathrm{d}x \end{aligned}$$

$$P_{\mathcal{R}_3} = \begin{cases} \dfrac{\Omega_2}{\Omega_1+\Omega_2} e^{-\epsilon_0 2^{r_0}\left(\frac{1}{\Omega_1}+\frac{1}{\Omega_2}\right)+\frac{\epsilon_0}{\Omega_1}} + \dfrac{\Omega_1}{\Omega_1+\Omega_2} e^{-\epsilon_0 2^{r_0}\left(\frac{1}{\Omega_1}+\frac{1}{\Omega_2}\right)+\frac{\epsilon_0}{\Omega_2}}, & \text{if } r_0 \geq 1, \\ \dfrac{\Omega_1}{\Omega_1+\Omega_2(2^{r_0}-1)} e^{-\epsilon_0\left(\frac{1}{\Omega_1}2^{r_0}+\frac{1}{\Omega_2}\right)} + \dfrac{\Omega_2}{\Omega_1(2^{r_0}-1)+\Omega_2} e^{-\epsilon_0\left(\frac{1}{\Omega_1}+\frac{1}{\Omega_2}2^{r_0}\right)} & \\ \quad - e^{-\left(\frac{1}{\Omega_1}+\frac{1}{\Omega_2}\right)\frac{\epsilon_0}{2-2^{r_0}}} \left[\dfrac{\Omega_2}{\Omega_1(2^{r_0}-1)+\Omega_2} - \dfrac{\Omega_2(2^{r_0}-1)}{\Omega_1+\Omega_2(2^{r_0}-1)} \right], & \text{if } r_0 < 1 \end{cases}$$

$$= e^{-\epsilon_0\left(\frac{1}{\Omega_1}+\frac{1}{\Omega_2}\right)} - e^{-\epsilon_0\left(\frac{1}{\Omega_2}+\frac{1}{\Omega_1}2^{r_0}\right)} + \frac{\Omega_2}{\Omega_1(2^{r_0}-1)+\Omega_2} e^{-\frac{\epsilon_0}{\Omega_2}} \left[e^{-\epsilon_0 2^{r_0}\left(\frac{1}{\Omega_1}+\frac{1}{\Omega_2}(2^{r_0}-1)\right)} - e^{-\epsilon_0\left(\frac{1}{\Omega_1}+\frac{1}{\Omega_2}(2^{r_0}-1)\right)} \right], \quad (15)$$

where $\zeta_2 \triangleq (2^{r_0}-1)x+\epsilon_0$. Similarly, we have

$$\begin{aligned} P_{\tilde{\mathcal{R}}_3^2} &= \int_{\epsilon_0 2^{r_0}}^{\zeta_3} \int_{\zeta_4}^{\zeta_2} \left(\frac{1}{\Omega_2} e^{-\frac{y}{\Omega_2}}\right)\left(\frac{1}{\Omega_1} e^{-\frac{x}{\Omega_1}}\right) \mathrm{d}y \mathrm{d}x \\ &= \int_{\epsilon_0 2^{r_0}}^{\zeta_3} \frac{1}{\Omega_1} e^{-\frac{x}{\Omega_1}} \left[e^{-\frac{1}{\Omega_2}\left(\frac{1}{2^{r_0}-1}x - \frac{\epsilon_0}{2^{r_0}-1}\right)} - e^{-\frac{1}{\Omega_2}((2^{r_0}-1)x+\epsilon_0)} \right] \mathrm{d}x \\ &= \left(\frac{\Omega_2(2^{r_0}-1)}{\Omega_1+\Omega_2(2^{r_0}-1)} e^{\frac{\epsilon_0}{\Omega_2(2^{r_0}-1)}}\right) \times \left[e^{-\left(\frac{1}{\Omega_1}+\frac{1}{\Omega_2(2^{r_0}-1)}\right)\epsilon_0 2^{r_0}} - e^{-\left(\frac{1}{\Omega_1}+\frac{1}{\Omega_2(2^{r_0}-1)}\right)\zeta_3} \right] \\ &\quad - \left(\frac{\Omega_2}{\Omega_1(2^{r_0}-1)+\Omega_2} e^{-\frac{1}{\Omega_2}\epsilon_0}\right) \times \left[e^{-\left(\frac{1}{\Omega_1}+\frac{(2^{r_0}-1)}{\Omega_2}\right)\epsilon_0 2^{r_0}} - e^{-\left(\frac{1}{\Omega_1}+\frac{(2^{r_0}-1)}{\Omega_2}\right)\zeta_3} \right], \end{aligned} \quad (16)$$

where $\zeta_3 \triangleq \frac{\epsilon_0 2^{r_0}}{1-(2^{r_0}-1)^2}$, and $\zeta_4 \triangleq \frac{x-\epsilon_0}{2^{r_0}-1}$.

Substituting (15) and (16) into (14), the expression of $P_{\tilde{\mathcal{R}}_3}$ can be obtained as shown in (7) for the case that $r_0 < 1$.

IV. HYBRID NOMA/OMA MODE SELECTION

The design of throughout-optimal buffer-aided relaying schemes for delay-constrained networks is still a challenging issue, which has not been solved even for the single-user case [13]. Alternatively, an efficient delay-constrained buffer-aided MS scheme will be proposed in this section.

TABLE 2. Weight for Each Mode, where $0 < \delta < 1/2$, $0 \ll \omega_1 \ll \omega_2 \ll \omega_3$.

Mode	Weight for each mode, i.e., W_k
$\mathcal{M}_1$	$\omega_1(L-l_1)$
$\mathcal{M}_2$	$\omega_1(L-l_2)+\delta$
$\mathcal{M}_3$	$\omega_2(L-\max\{l_1,l_2\})+\delta$
$\mathcal{M}_4$	$\omega_3(\min\{l_1,l_2\}-1)+\omega_2$
$\mathcal{M}_5$	2δ

The basic idea is to allocate each mode $\mathcal{M}_k$ a weight, denoted by W_k, to determine the priority of each mode, which is given in Table 2, where $0 < \delta < 1/2$ is used to differentiate two weights with the same integer part. In addition, ω_1, ω_2 and ω_3 in Table 2 are used to denote three different priority layers of the transmission modes, where $0 \ll \omega_1 \ll \omega_2 \ll \omega_3$. In particular, when $\min\{l_1, l_2\} \geq 2$, $\mathcal{M}_4$ lies on layer ω_3, which enjoys the highest priority. The motivation of the threshold of 2 is to achieve the tradeoff between outage probability minimization and average packet delay minimization [24], [34]. In this case, each buffer will be prone to remain at the size of 1 or 2 especially at high SNR, which means that each buffer is neither full nor empty in most time slots as long as $L \geq 3$. When $\min\{l_1, l_2\} = 1$, $\mathcal{M}_4$ falls down to layer ω_2, the same layer with $\mathcal{M}_3$. Moreover, the OMA modes $\mathcal{M}_1$ and $\mathcal{M}_2$ lies in layer ω_1, and the silent mode $\mathcal{M}_5$ will be selected only if the weight of any other mode is smaller than 2δ or its CSI requirement is not satisfied.

With the allocated weights, the hybrid NOMA/OMA based MS scheme can be mathematically expressed as follows. In particular, mode $\mathcal{M}_{k^*}$ is selected in each time slot, where k^* is given by

$$k^* = \arg \max_{k \in \mathcal{R}_k, W_k \geq 2\delta} W_k. \quad (17)$$

Remark 3: Hybrid NOMA/OMA will reduce to NOMA, if we disable the transmission mode $\mathcal{M}_1$ and $\mathcal{M}_2$ by setting $W_1 = W_2 = 0$, i.e., only modes $\mathcal{M}_3$ and $\mathcal{M}_4$ are used to receive and transmit messages at the relay, respectively. In addition, if we disable mode $\mathcal{M}_3$ by setting $W_3 = 0$, hybrid NOMA/OMA will reduce to OMA where the users transmit messages to the relay in orthogonal time slots.

V. PERFORMANCE OF BUFFER-AIDED HYBRID NOMA/OMA

In this section, the performance of the proposed buffer-aided hybrid NOMA/OMA scheme will be analyzed by formulating a MC as well as its transition matrix to model the evolution of the relay buffers.

A. STATE TRANSMISSION MATRIX

Let $s_n = (l_1, l_2), n \in \{1, 2, \ldots, (L+1)^2\}$, denote the states in the MC, which describes the queues of the two buffers at the relay. Let $\mathbf{A}$ denote the $(L+1)\times(L+1)$ state transition matrix, whose entry $\mathbf{A}_{i,j} = p(s_j \to s_i) = \mathbb{P}\{(l_1(t+1), l_2(t+1)) = s_i | (l_1(t), l_2(t)) = s_j\}$ is the transition probability to move from state s_j at time t to s_i at time $t+1$. The transition probabilities for the proposed scheme can be summarized in the following proposition.

Proposition 2: The transition probabilities of the states of the MC for the proposed hybrid NOMA/OMA based MS scheme are given in (19)–(23), as shown at the bottom of the next page, where "$\vee$" and "$\wedge$" denote "or" and "and", respectively. In addition, $P_{\mathcal{R}_k}$ denotes the probability that the channel gains lie in the region $\mathcal{R}_k$ shown in Table 1, $k \in \{1, 2, 3, 4\}$. Specifically, $P_{\mathcal{R}_1} = e^{-\frac{\epsilon_0}{\Omega_1}}$, $P_{\mathcal{R}_2} = e^{-\frac{\epsilon_0}{\Omega_2}}$, and $P_{\mathcal{R}_4} = e^{-\frac{\epsilon_R}{\Omega_R}}$, and $P_{\mathcal{R}_3}$ is given in (4) and (7) for the scenarios with dynamic and fixed PCs, respectively.

Proof 2: Please refer to Appendix A.

When the buffer size $L = 2$, there are $(L+1)\times(L+1) = 9$ buffer states in total and the state MC for $L = 2$ is presented in Fig. 5. According to Proposition 2, the corresponding state transition matrix A for $L = 2$ can be written as (18) at the bottom of the next page.

B. PERFORMANCE OF THE PROPOSED SCHEME

One can verify that the transition matrix $\mathbf{A}$ is column stochastic and irreducible,[3] so the stationary state probability vector can be obtained as follows [20]:

$$\boldsymbol{\pi} = (\mathbf{A} - \mathbf{I} + \mathbf{B})^{-1}\mathbf{b}, \tag{25}$$

where $\boldsymbol{\pi} = [\pi_{s_1}, \cdots, \pi_{s_{(L+1)^2}}]^T$, $\mathbf{b} = [1, 1, \cdots, 1]^T$ and $\mathbf{B}_{i,j} = 1, \forall i, j$. In the next, we will use $\pi_{(l_1,l_2)}$ to denote the

[3]Column stochastic means that all entries in any column sum up to one; irreducible means that it is possible to move from any state to any state [35].

$$\mathbf{A} = \begin{Bmatrix}
\bar{P}_{\mathcal{R}_1}\bar{P}_{\mathcal{R}_2} & 0 & 0 & 0 & \bar{P}_{\mathcal{R}_3}P_{\mathcal{R}_4} & 0 & 0 & 0 & 0 \\
P_{\mathcal{R}_2} - P_{\mathcal{R}_3} & \bar{P}_{\mathcal{R}_1}\bar{P}_{\mathcal{R}_2} & 0 & 0 & 0 & P_{\mathcal{R}_4} & 0 & 0 & 0 \\
0 & \bar{P}_{\mathcal{R}_1}P_{\mathcal{R}_2} & \bar{P}_{\mathcal{R}_1} & 0 & 0 & 0 & 0 & 0 & 0 \\
P_{\mathcal{R}_1}\bar{P}_{\mathcal{R}_2} & 0 & 0 & \bar{P}_{\mathcal{R}_1}\bar{P}_{\mathcal{R}_2} & 0 & 0 & 0 & P_{\mathcal{R}_4} & 0 \\
P_{\mathcal{R}_3} & P_{\mathcal{R}_1} - P_{\mathcal{R}_3} & 0 & P_{\mathcal{R}_2} - P_{\mathcal{R}_3} & \bar{P}_{\mathcal{R}_1}\bar{P}_{\mathcal{R}_2}\bar{P}_{\mathcal{R}_4} & 0 & 0 & 0 & P_{\mathcal{R}_4} \\
0 & P_{\mathcal{R}_3} & P_{\mathcal{R}_1} & 0 & (P_{\mathcal{R}_2} - P_{\mathcal{R}_3})\bar{P}_{\mathcal{R}_4} & \bar{P}_{\mathcal{R}_1}\bar{P}_{\mathcal{R}_4} & 0 & 0 & 0 \\
0 & 0 & 0 & P_{\mathcal{R}_1}\bar{P}_{\mathcal{R}_2} & 0 & 0 & \bar{P}_{\mathcal{R}_2} & 0 & 0 \\
0 & 0 & 0 & P_{\mathcal{R}_3} & P_{\mathcal{R}_1}\bar{P}_{\mathcal{R}_2}\bar{P}_{\mathcal{R}_4} & 0 & P_{\mathcal{R}_2} & \bar{P}_{\mathcal{R}_2}\bar{P}_{\mathcal{R}_4} & 0 \\
0 & 0 & 0 & 0 & P_{\mathcal{R}_3} & P_{\mathcal{R}_1}\bar{P}_{\mathcal{R}_4} & 0 & P_{\mathcal{R}_2}\bar{P}_{\mathcal{R}_4} & \bar{P}_{\mathcal{R}_4}
\end{Bmatrix} \tag{18}$$

$$P_{(l_1,l_2)}^{(l_1',l_2')} = 0, \quad \text{if } |l_1' - l_1| \geq 2 \vee |l_2' - l_2| \geq 2 \vee \{l_1' = l_1 - 1 \wedge l_2' \neq l_2 - 1\} \vee \{l_1' \neq l_1 - 1 \wedge l_2' = l_2 - 1\}. \tag{19}$$

$$P_{(l_1,l_2)}^{(l_1,l_2)} = \begin{cases}
(1 - P_{\mathcal{R}_1})(1 - P_{\mathcal{R}_2})(1 - P_{\mathcal{R}_4}) & \text{if } \max\{l_1, l_2\} < L \wedge \min\{l_1, l_2\} > 0, \\
(1 - P_{\mathcal{R}_1})(1 - P_{\mathcal{R}_2}) & \text{if } \max\{l_1, l_2\} < L \wedge \min\{l_1, l_2\} = 0, \\
(1 - P_{\mathcal{R}_2})(1 - P_{\mathcal{R}_4}) & \text{if } l_1 = L \wedge 0 < l_2 < L, \\
(1 - P_{\mathcal{R}_1})(1 - P_{\mathcal{R}_4}) & \text{if } l_2 = L \wedge 0 < l_1 < L, \\
1 - P_{\mathcal{R}_1} & \text{if } l_1 = 0 \wedge l_2 = L, \\
1 - P_{\mathcal{R}_2} & \text{if } l_2 = 0 \wedge l_1 = L, \\
1 - P_{\mathcal{R}_4} & \text{if } l_1 = l_2 = L, \\
0 & \text{otherwise}
\end{cases} \tag{20}$$

$$P_{(l_1,l_2)}^{(l_1+1,l_2)} = \begin{cases}
P_{\mathcal{R}_1}(1 - P_{\mathcal{R}_2})(1 - P_{\mathcal{R}_4}) & \text{if } 0 < l_2 \leq l_1 < L, \\
\left(P_{\mathcal{R}_1} - P_{\mathcal{R}_3}\right)(1 - P_{\mathcal{R}_4}) & \text{if } 0 < l_1 < l_2 < L, \\
P_{\mathcal{R}_1}(1 - P_{\mathcal{R}_4}) & \text{if } 0 < l_1 < l_2 = L, \\
P_{\mathcal{R}_1}(1 - P_{\mathcal{R}_2}) & \text{if } 0 = l_2 \leq l_1 < L, \\
P_{\mathcal{R}_1} - P_{\mathcal{R}_3} & \text{if } 0 = l_1 < l_2 < L, \\
P_{\mathcal{R}_1} & \text{if } l_1 = 0, l_2 = L, \\
0 & \text{otherwise}
\end{cases} \tag{21}$$

$$P_{(l_1,l_2)}^{(l_1,l_2+1)} = \begin{cases}
\left(P_{\mathcal{R}_2} - P_{\mathcal{R}_3}\right)(1 - P_{\mathcal{R}_4}) & \text{if } 0 < l_2 \leq l_1 < L, \\
P_{\mathcal{R}_2}(1 - P_{\mathcal{R}_1})(1 - P_{\mathcal{R}_4}) & \text{if } 0 < l_1 < l_2 < L, \\
P_{\mathcal{R}_2}(1 - P_{\mathcal{R}_4}) & \text{if } 0 < l_2 < l_1 = L, \\
P_{\mathcal{R}_2}(1 - P_{\mathcal{R}_1}) & \text{if } 0 = l_1 < l_2 < L, \\
P_{\mathcal{R}_2} - P_{\mathcal{R}_3} & \text{if } 0 = l_2 \leq l_1 < L, \\
P_{\mathcal{R}_2} & \text{if } l_1 = L, l_2 = 0, \\
0 & \text{otherwise}
\end{cases} \tag{22}$$

$$P_{(l_1,l_2)}^{(l_1+1,l_2+1)} = \begin{cases}
(1 - P_{\mathcal{R}_4})\, P_{\mathcal{R}_3} & \text{if } \max\{l_1, l_2\} < L \wedge \min\{l_1, l_2\} \geq 2, \\
P_{\mathcal{R}_3} & \text{if } \max\{l_1, l_2\} < L \wedge \min\{l_1, l_2\} < 2, \\
0 & \text{otherwise}
\end{cases} \tag{23}$$

$$P_{(l_1,l_2)}^{(l_1-1,l_2-1)} = \begin{cases}
P_{\mathcal{R}_4}(1 - P_{\mathcal{R}_3}) & \text{if } \max\{l_1, l_2\} < L \wedge \min\{l_1, l_2\} = 1, \\
P_{\mathcal{R}_4} & \text{if } \min\{l_1, l_2\} \geq 2 \vee \{\min\{l_1, l_2\} = 1 \wedge \max\{l_1, l_2\} = L\}, \\
0 & \text{otherwise}
\end{cases} \tag{24}$$

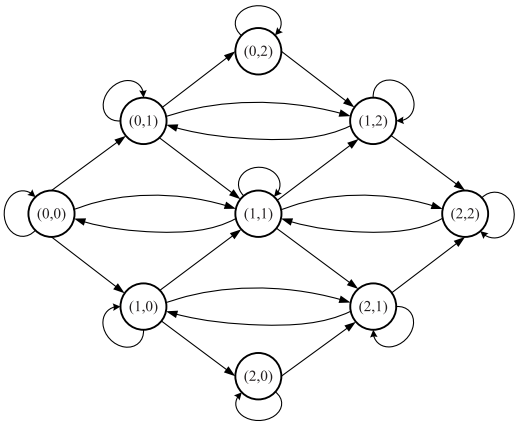

FIGURE 5. Markov chain representing the states of the buffers size $L = 2$.

stationary state probability of the buffer state $s_n = (l_1, l_2)$ for simplicity.

In the following, the performance of the sum throughput, the outage probability, and the average packet delay will be analyzed.

1) THROUGHPUT

Over a long time of period, obviously the sum receive and the transmit throughputs at the relay will be the same, and the sum throughput of the system can be expressed as follows:

$$\begin{aligned}\bar{R}_{sum} &= r_0 \sum_{l_1=0}^{L-1}\sum_{l_2=0}^{L-1}(P_{(l_1,l_2)}^{(l_1+1,l_2)}+P_{(l_1,l_2)}^{(l_1,l_2+1)}+2P_{(l_1,l_2)}^{(l_1+1,l_2+1)})\pi_{(l_1,l_2)} \\ &= 2r_0 \sum_{l_1=1}^{L}\sum_{l_2=1}^{L} P_{(l_1,l_2)}^{(l_1-1,l_2-1)}\pi_{(l_1,l_2)}. \end{aligned} \tag{26}$$

2) OUTAGE PROBABILITY

Since the target sum rate is r_0 BPCU ($r_0/2$ BPCU for each user), the outage probability of the system can be expressed as follows:

$$P_{sys}^{out} = 1 - \frac{\bar{R}_{sum}}{r_0}. \tag{27}$$

Based on the system outage probability P_{sys}^{out}, the diversity gain of the proposed hybrid NOMA scheme is defined as follows:

$$d_0 \triangleq -\lim_{\rho\to\infty} \frac{\log P_{sys}^{out}}{\log \rho}. \tag{28}$$

Proposition 3: The diversity gain of 2 can be achieved by the proposed hybrid NOMA scheme in both the scenarios of dynamic and fixed PCs at the users, i.e., $d_0 = 2$, as long as $L \geq 3$.

Proof 3: Please refer to Appendix B.

Proposition 3 implies that fixed PC will not lead to a loss of diversity gain in comparison with dynamic PC, using the proposed design of the transmit power at each user in (6).

3) AVERAGE PACKET DELAY

Denote P_k as the probability that mode $\mathcal{M}_k$ is selected. Over a long period of time, based on (26), we obtain

$$P_1 + P_2 + 2P_3 = 2P_4 = 1 - P_{sys}^{out}. \tag{29}$$

Moreover, denote η_U and η_R as the transmit sum throughputs (in number of packets per time slot) of the users and the relay, respectively, which can be expressed as

$$\eta_U = \eta_R = \frac{\bar{R}_{sum}}{r_0} = 1 - P_{sys}^{out}. \tag{30}$$

Since in each time slot, at most two packets are transmitted from the two users, the average sum queuing length (in number of time slots) at two users can be obtained as

$$Q_U = 2 - (P_1 + P_2 + 2P_3) = 1 + P_{sys}^{out}. \tag{31}$$

Thus, the average packet delay at the two users is

$$D_U = \frac{Q_U}{\eta_U} = \frac{1 + P_{sys}^{out}}{1 - P_{sys}^{out}}. \tag{32}$$

In addition, the average packet delay at the relay is $D_R = \bar{Q}_R/\eta_R$, where $\bar{Q}_R$ is the average sum queuing length of the two buffers, which can be expressed as

$$\bar{Q}_R = \sum_{l_1=0}^{L}\sum_{l_2=0}^{L}(l_1 + l_2)\pi_{(l_1,l_2)}. \tag{33}$$

In summary, the total average packet delay of the system is $D_U + D_R$.

VI. NUMERICAL RESULTS

In this section, we evaluate the performance of the proposed hybrid NOMA/OMA based MS scheme by using computer simulations, in terms of sum throughput, outage probability and average packet delay. Furthermore, asymmetric distances are considered, which are set as $d_1 = 1$, $d_2 = 2$ and $d_R = 1$, and the path loss exponent is chosen as $\gamma = 2$ to reflect a favorable propagation condition. This means that $\Omega_1 = 1$, $\Omega_2 = \frac{1}{4}$, and $\Omega_R = 1$. In the following subsections, we present the performance of the proposed hybrid NOMA/OMA scheme in two scenarios of dynamic and fixed PCs at users.

A. DYNAMIC POWER CONTROL

In this subsection, Figs. 6–9 are provided to compare the performance of the proposed hybrid NOMA/OMA scheme and the conventional NOMA and OMA schemes, where it is assumed that dynamic PC is adopted at the users for all the schemes.

In Fig. 6, sum throughput comparison is presented for the proposed hybrid NOMA/OMA scheme and the conventional NOMA and OMA schemes, where the buffer size is set as $L = 5$. One can observe that, when $r_0 = 2$ BPCU, the hybrid NOMA/OMA and NOMA schemes achieve the maximum sum throughput of 2 BPCU at high SNR, whereas the OMA scheme can only achieve about 1.3 BPCU in this case.

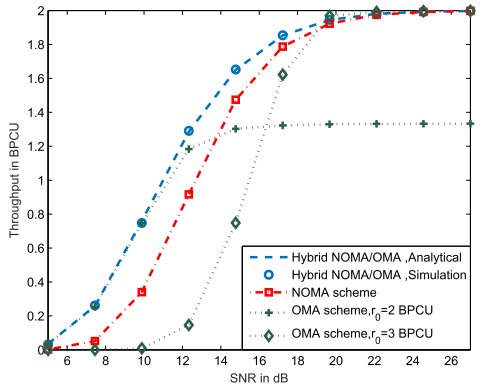

FIGURE 6. Sum throughput vs. transmit SNR, where $L = 5$.

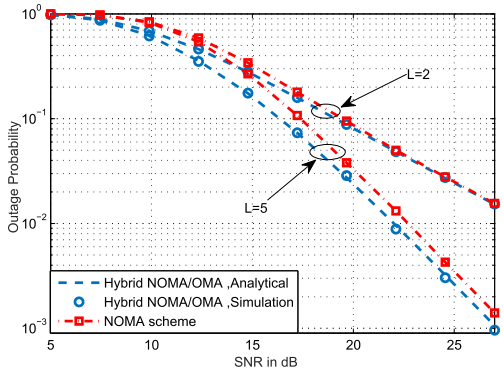

FIGURE 7. System outage probability vs. transmit SNR, where $r_0 = 2$ BPCU.

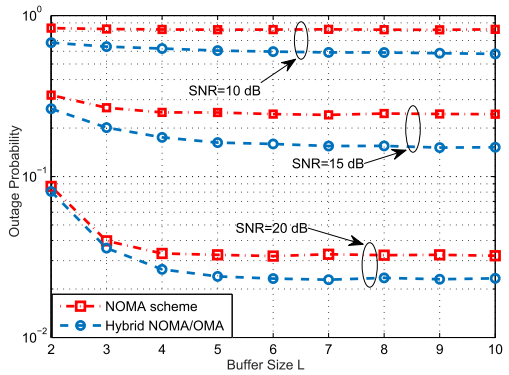

FIGURE 8. System outage probability vs. buffer size L, where $r_0 = 2$ BPCU.

This is because only one packet can be transmitted from the users to the relay in one time slot for the OMA scheme. If we set $r_0 = 3$ BPCU, OMA can achieve the sum throughput of 2 BPCU at high SNR, but have a poor performance at low or moderate SNR. In addition, the proposed hybrid NOMA/OMA scheme outperforms the comparative ones significantly.

The outage probability performance of the proposed hybrid NOMA/OMA scheme and the NOMA scheme are presented in Figs. 7 and 8 versus SNR and buffer size L, respectively. It can be seen from Fig. 7 that the gap between the two schemes is slight when $L = 2$, especially at high SNR, but significant performance gap exists when $L = 5$. In Fig. 8, one

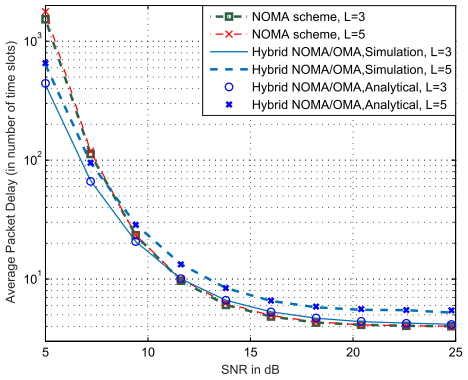

FIGURE 9. Average packet delay vs. transmit SNR, where $r_0 = 2$ BPCU.

can observe that the proposed hybrid NOMA/OMA scheme achieves lower outage probability compared to the NOMA scheme for different buffer sizes and SNRs. In particular, the proposed scheme can benefit from enlarging L significantly, whereas the outage probability of the NOMA scheme almost does not decrease when $L \geq 5$.

In Fig. 9, we present average packet delay comparison of the proposed hybrid NOMA/OMA scheme and the NOMA scheme when $L = 3$ and $L = 5$. We observe that, at low SNR, the proposed hybrid NOMA/OMA scheme achieves a much shorter average packet delay than NOMA scheme. This is because the average packet delay at the users is the dominant factor when the outage probability is high at low SNR (shown in Section V-B). At high SNR, the proposed scheme suffers from a longer average packet delay especially when $L = 5$. This is because the average packet delay at the relay is the dominant factor at high SNR. For the proposed scheme, a single packet is transmitted when an OMA transmission mode ($\mathcal{M}_1$ or $\mathcal{M}_2$) is selected, which may obstruct the following received packets in the same buffer. However, it can be seen that the average packet delay of the proposed scheme is just slightly longer than the NOMA scheme at high SNR.

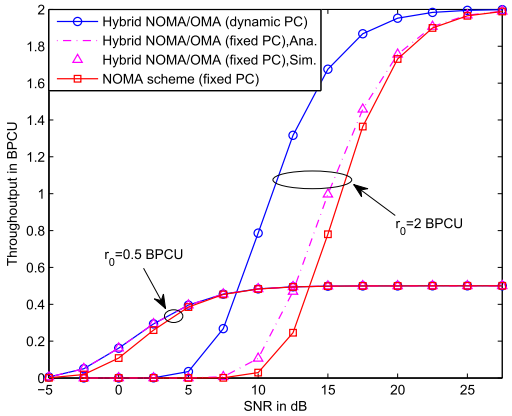

FIGURE 10. Sum throughput vs. transmit SNR, where $L = 5$.

B. FIXED POWER CONTROL

In this subsection, Figs. 10–13 are provided to compare the performance of the proposed hybrid NOMA/OMA scheme

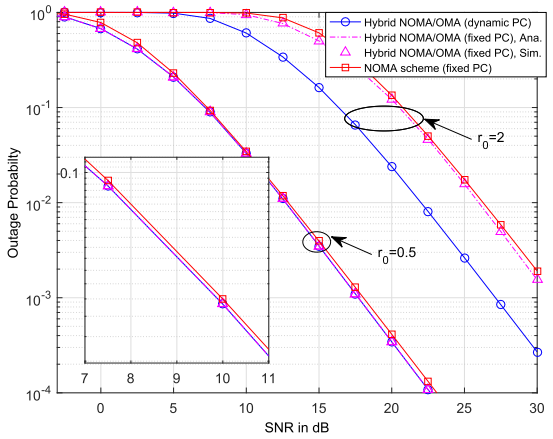

FIGURE 11. System outage probability vs. transmit SNR, where $L = 5$.

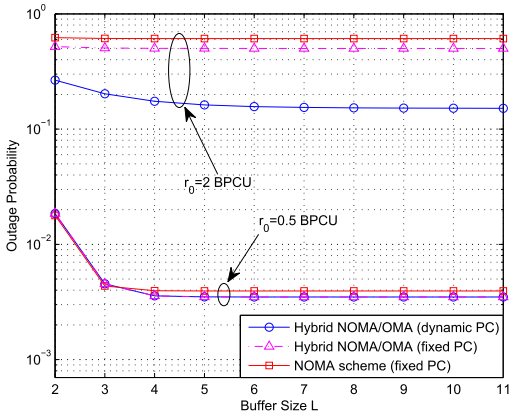

FIGURE 12. System outage probability vs. buffer size L, where SNR= 15 dB.

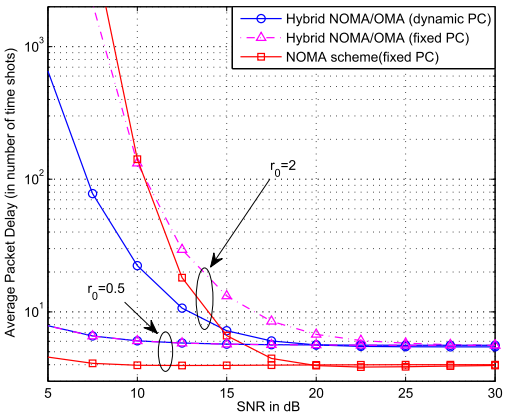

FIGURE 13. Average packet delay vs. transmit SNR, where $L = 5$.

and the conventional NOMA scheme, in the scenario of the fixed PC at the users. The hybrid NOMA/OMA scheme with dynamic PC is also depicted as an upper bound for the proposed scheme with fixed PC.

In Fig. 10, with the fixed PC, hybrid NOMA/OMA significantly outperforms the conventional NOMA, in terms of sum throughput. When the transmit rate $r_0 = 2$ BPCU, hybrid NOMA/OMA scheme with fixed PC performs worse than hybrid NOMA/OMA scheme with dynamic PC, which can be explained by the fact that the required NOMA region $\mathcal{R}_3$ for dynamic PC in Fig. 2 has a much lager domain than that for fixed PC in Fig. 3. While when the transmit rate $r_0 = 0.5$ BPCU, hybrid NOMA/OMA with fixed PC can achieve almost the same sum throughput as hybrid NOMA/OMA with dynamic PC. This is because when the transmission rate is small, there is only a little difference between the required NOMA region $\mathcal{R}_3$ for dynamic PC in Fig. 2 and that for fixed PC in Fig. 4.

Fig. 11 shows the outage probability, P_{sys}^{out}, for the hybrid NOMA/OMA and NOMA schemes. Hybrid NOMA/OMA also outperforms NOMA especially when $r_0 = 2$ BPCU. The outage probability performance of hybrid NOMA/OMA with dynamic PC performance better than hybrid NOMA/OMA scheme with fixed PC, when the transmit rate $r_0 = 2$ BPCU. However, one can observe that the advantage of hybrid NOMA/OMA with dynamic PC narrows compared to hybrid NOMA/OMA with fixed PC, when the transmit rate reduces to 0.5 BPCU.

In Fig. 12, we depict the outage probability P_{sys}^{out} for the corresponding three schemes as a function of the buffer size L, in order to consider the impact of the buffer size L. Obviously, the outage probability for each scheme decreases with L. Furthermore, when $r_0 = 2$ BPCU, it can be seen that the outage probabilities of the both the hybrid NOMA/OMA and NOMA schemes with fixed PC changes little for the region $L \geq 2$, while the curve of hybrid NOMA/OMA with dynamic PC almost keeps unchanged for the region $L \geq 6$. When $r_0 = 0.5$ BPCU, the performance of each scheme keeps unchanged for the region $L \geq 4$. Thus, it is suitable for the proposed hybrid NOMA/OMA scheme to choose a small buffer size of L between 3 and 5.

In Fig. 13, we present the average packet delay in number of time shots of three schemes versus the SNR. We note that, when the transmit rate $r_0 = 2$ BPCU, the average packet delay of hybrid NOMA/OMA with fixed PC is longer than that with dynamic PC at low SNR, because the delay at the users is the dominant factor in this case. However, when $r_0 = 0.5$ BPCU, the delay of hybrid NOMA/OMA scheme with fixed PC is almost the same as that with dynamic PC. In addition, similar to Fig. 9, the conventional NOMA scheme achieves a shorter average packet delay at high SNR, and the performance gain is about 1.5 time slots compared to hybrid NOMA/OMA.

VII. CONCLUSION

This paper investigated a cooperative uplink system with two users, a buffer-aided relay, and a BS. A hybrid NOMA/OMA based MS scheme has been proposed, which adaptively switches between the NOMA and OMA transmission modes according to the instantaneous CSI and buffer state. We have derived the probability for the user-to-relay channels to successfully perform NOMA in two scenarios of dynamic and fixed PCs at users. Accordingly, we carefully designed the transmit power at users such that the inter-user interference

can be controlled. Then, we have analyzed the state transmission matrix probabilities of the corresponding MC, and derived closed-form expressions for sum throughput, outage probability, and average packet delay. A diversity gain of two was proved to be achieved when the buffer size is not smaller than three for both dynamic and fixed PCs. Numerical results have shown that the proposed hybrid NOMA/OMA scheme with dynamic PC significantly outperforms the conventional NOMA and OMA schemes in most scenarios.

APPENDIXES

APPENDIX A

PROOF OF PROPOSITION 2

To prove this proposition, we first analyze the probability of the required CSI region for each mode $\mathcal{M}_k$ (shown in Table 1), denoted by $P_{\mathcal{R}_k}$, $k \in \{1, 2, 3, 4\}$ where $P_{\mathcal{R}_3}$ is given in (4) and (7) for dynamic and fixed PCs, respectively, and the other probabilities can be easily given as follows:

$$P_{\mathcal{R}_1} = e^{-\frac{\epsilon_0}{\Omega_1}}, \quad P_{\mathcal{R}_2} = e^{-\frac{\epsilon_0}{\Omega_2}}, \; P_{\mathcal{R}_4} = e^{-\frac{\epsilon_R}{\Omega_R}}. \tag{34}$$

We then consider the following cases:

1) Since each buffer at most receives or transmits only one packet in one time slot, $P_{(l_1,l_2)}^{(l_1',l_2')} = 0$ if $|l_u' - l_u| \geq 2$, $u = 1, 2$. Moreover, two buffers transmit at the same time slot in the proposed scheme, and hence (19) can be easily obtained.
2) $P_{(l_1,l_2)}^{(l_1,l_2)}$ corresponds to the case that mode $\mathcal{M}_5$ is selected, which is shown in (20). Since weight W_5 has the smallest value when $\max\{l_1, l_2\} < L \wedge \min\{l_1, l_2\} > 0$ compared to the other modes' weights, mode $\mathcal{M}_5$ can only be selected if all channels are so weak that the other modes' CSI requirements (shown in Table 1) cannot be satisfied. In this subcase, $P_{(l_1,l_2)}^{(l_1,l_2)} = (1 - P_{\mathcal{R}_1})(1 - P_{\mathcal{R}_2})(1 - P_{\mathcal{R}_4})$. When $\max\{l_1, l_2\} < L \wedge \min\{l_1, l_2\} = 0$, the buffer requirement of mode $\mathcal{M}_4$ cannot be satisfied, i.e., we do not need to consider the CSI requirement of the mode $\mathcal{M}_4$. Furthermore, if the CSI requirements of modes $\mathcal{M}_1$, $\mathcal{M}_2$ and $\mathcal{M}_3$ either cannot be satisfied, we can only choose mode $\mathcal{M}_5$, and $P_{(l_1,l_2)}^{(l_1,l_2)} = (1 - P_{\mathcal{R}_1})P_{\mathcal{R}_2}$. When $l_1 = L \wedge 0 < l_2 < L$, mode $\mathcal{M}_1$ cannot satisfy the buffer requirement, so in this subcases, $P_{(l_1,l_2)}^{(l_1,l_2)} = (1 - P_{\mathcal{R}_2})(1 - P_{\mathcal{R}_4})$. Similarly, when $l_2 = L \wedge 0 < l_1 < L$, we obtained $P_{(l_1,l_2)}^{(l_1,l_2)} = (1 - P_{\mathcal{R}_1})(1 - P_{\mathcal{R}_4})$. When one buffer is full while the other is empty, the buffer requirements of modes $\mathcal{M}_3$ and $\mathcal{M}_4$ cannot be satisfied, hence we can only choose mode $\mathcal{M}_5$ if the CSI of the channel linked to empty buffer is either poor. So we can easily derive that $P_{(l_1,l_2)}^{(l_1,l_2)} = (1 - P_{\mathcal{R}_1})$ when $l_1 = 0 \wedge l_2 = L$, $P_{(l_1,l_2)}^{(l_1,l_2)} = (1 - P_{\mathcal{R}_2})$ when $l_2 = 0 \wedge l_1 = L$. When $l_1 = l_2 = L$, only $\mathcal{M}_4$'s buffer requirement is satisfied. So when it's CSI requirement cannot be satisfied, the system can only keep silent and $P_{(l_1,l_2)}^{(l_1,l_2)} = (1 - P_{\mathcal{R}_4})$.
3) $P_{(l_1,l_2)}^{(l_1+1,l_2)}$ corresponds to the case that mode $\mathcal{M}_1$ is selected, which is shown in (21). In the subcase where $0 < l_2 \leq l_1 < L$, $W_5 < W_1 < \min\{W_2, W_3, W_4\}$, so mode $\mathcal{M}_1$ can be selected only if the CSI requirement of $\mathcal{M}_1$ can be satisfied but the CSI requirement of $\mathcal{M}_i$ cannot be satisfied, $i = 2, 3, 4$, and thus $P_{(l_1,l_2)}^{(l_1+1,l_2)} = P_{\mathcal{R}_1}(1 - P_{\mathcal{R}_2})(1 - P_{\mathcal{R}_4})$. However, when $0 < l_1 < l_2 < L$, $W_5 < W_2 < W_1 < \min\{W_3, W_4\}$, so we need not consider mode $\mathcal{M}_2$. From Fig. 2, Fig. 4 and Fig. 3, we can derive that $P_{(l_1,l_2)}^{(l_1+1,l_2)} = (P_{\mathcal{R}_1} - P_{\mathcal{R}_3})(1 - P_{\mathcal{R}_4})$. Moreover, when $0 < l_1 < l_2 = L$, $W_3 < W_5 < W_2 < W_1 < W_4$, then $P_{(l_1,l_2)}^{(l_1+1,l_2)} = P_{\mathcal{R}_1}(1 - P_{\mathcal{R}_4})$. In the subcase $0 = l_2 \leq l_1 < L$, $W_4 < W_5 < W_1 < \min\{W_2, W_3\}$, so if the CSI requirement of modes $\mathcal{M}_2$ and $\mathcal{M}_3$ cannot be satisfied, we will choose mode $\mathcal{M}_3$, $P_{(l_1,l_2)}^{(l_1+1,l_2)} = P_{\mathcal{R}_1}(1 - P_{\mathcal{R}_2})$. When $0 = l_1 < l_2 < L$, $W_4 < W_5 < W_2 < W_1 < W_3$, we can only choose mode $\mathcal{M}_1$ if the CSI requirement of mode $\mathcal{M}_3$ cannot be satisfied, then we obtained that $P_{(l_1,l_2)}^{(l_1+1,l_2)} = P_{\mathcal{R}_1}(1 - P_{\mathcal{R}_3})$. When $0 = l_1 \wedge l_2 = L$, mode $\mathcal{M}_1$ has the max weight and deserves the highest priority, so we will choose the user 1 to transmit if mode $\mathcal{M}_1$'s CSI is available. Furthermore, we can obtain that $P_{(l_1,l_2)}^{(l_1+1,l_2)} = P_{\mathcal{R}_1}$.
4) $P_{(l_1,l_2)}^{(l_1+1,l_2+1)}$ corresponds to the case that mode $\mathcal{M}_3$ is selected. If $\max\{l_1, l_2\} < L \wedge \min\{l_1, l_2\} = 2$, $W_3 > W_i$, $i = 1, 2, 5$, and $W_3 < W_4$, so mode $\mathcal{M}_3$ can be selected only if the CSI requirement of $\mathcal{M}_3$ can be satisfied but the CSI requirement of $\mathcal{M}_4$ cannot be satisfied, and thus $P_{(l_1,l_2)}^{(l_1+1,l_2+1)} = P_{\mathcal{R}_3}(1 - P_{\mathcal{R}_4})$. If $\max\{l_1, l_2\} < L \wedge \min\{l_1, l_2\} < 2$, W_3 has the largest value, and hence $P_{(l_1,l_2)}^{(l_1+1,l_2+1)} = P_{\mathcal{R}_3}$.
5) $P_{(l_1,l_2)}^{(l_1-1,l_2-1)}$ corresponds to the case that mode $\mathcal{M}_4$ is selected, and (23) can be easily obtained, following similar derivation steps for the pervious case. If $\max\{l_1, l_2\} < L \wedge \min\{l_1, l_2\} = 1$, $W_4 > W_i$, $i = 1, 2, 5$, and $W_4 < W_3$, so mode $\mathcal{M}_4$ can be selected only if the CSI requirement of $\mathcal{M}_4$ can be satisfied but the CSI requirement of $\mathcal{M}_3$ cannot be satisfied, and thus $P_{(l_1,l_2)}^{(l_1-1,l_2-1)} = P_{\mathcal{R}_4}(1 - P_{\mathcal{R}_3})$. If $\min\{l_1, l_2\} \geq 2 \vee \{\min\{l_1, l_2\} = 1 \wedge \max\{l_1, l_2\} = L\}$, W_4 has the largest value, and hence $P_{(l_1,l_2)}^{(l_1-1,l_2-1)} = P_{\mathcal{R}_4}$.

APPENDIX B

PROOF OF PROPOSITION 3

The transition matrix $\mathbf{A}$ is too complicated (shown in Proposition 1) to obtain an explicit approximation of the outage probability P_{sys}^{out} in (7) at high SNR. Alternatively, we wish to derive an upper bound on P_{sys}^{out} in order to obtain an achievable diversity gain of the proposed scheme. In particular, it should be noted that the throughput achieved by the NOMA scheme (mentioned in Remark 3) is just a lower bound of the proposed hybrid NOMA/OMA scheme. This is because the relay can still receive messages by using modes $\mathcal{M}_1$ and $\mathcal{M}_2$ for the proposed hybrid NOMA/OMA scheme, even if the CSI requirements of $\mathcal{M}_3$ and $\mathcal{M}_4$ cannot be satisfied.

Thus, the outage probability of the NOMA scheme, denoted by P_N^{out}, is an upper bound of P_{sys}^{out}.

Using the NOMA scheme, there exists only three modes ($\mathcal{M}_k$, $k = \{3, 4, 5\}$) and $(L+1)$ states since the two buffers have the same size in each time slot. The MC of the simplified NOMA scheme for the case $L = 3$ is presented in Fig. 14, where each transition probability from state i to state j, denoted by P_i^j.

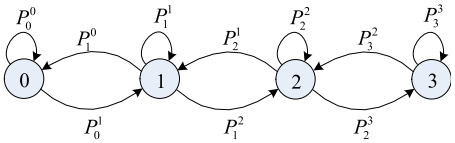

FIGURE 14. Diagram of the MC of the simplified NOMA scheme with $L = 3$.

In the following, each transition probability will be approximated in both the scenarios of dynamic and fixed PCs at the users, so that the steady probabilities can also be approximated at high SNR and the achievable diversity gain can be achieved.

A. DYNAMIC POWER CONTROL

Based on $P_{\mathcal{R}_3}$ in (4) for dynamic PC and $P_{\mathcal{R}_4}$ in (34), each transition probability can be easily approximated as

$$P_0^0 = 1 - P_{\mathcal{R}_3} \approx \epsilon_0 \left(\frac{1}{\Omega_1} + \frac{1}{\Omega_2}\right), \tag{35}$$

$$P_1^1 = P_2^2 = (1 - P_{\mathcal{R}_3})(1 - P_{\mathcal{R}_4}) \approx \frac{\epsilon_0 \epsilon_R}{\Omega_R} \left(\frac{1}{\Omega_1} + \frac{1}{\Omega_2}\right), \tag{36}$$

$$P_3^3 = 1 - P_{\mathcal{R}_4} \approx \frac{\epsilon_R}{\Omega_R}, \tag{37}$$

$$P_0^1 = P_1^2 = P_{\mathcal{R}_3} \approx 1 - \epsilon_0 \left(\frac{1}{\Omega_1} + \frac{1}{\Omega_2}\right), \tag{38}$$

$$P_2^3 = P_{\mathcal{R}_3}(1 - P_{\mathcal{R}_4}) \approx \frac{\epsilon_R}{\Omega_R}, \tag{39}$$

$$P_3^2 = P_2^1 = P_{\mathcal{R}_4} \approx 1 - \frac{\epsilon_R}{\Omega_R}, \tag{40}$$

$$P_1^0 = P_{\mathcal{R}_4}(1 - P_{\mathcal{R}_3}) \approx \epsilon_0 \left(\frac{1}{\Omega_1} + \frac{1}{\Omega_2}\right), \tag{41}$$

at high SNR, by using Taylor expansion. Based on the above transition probabilities, the stationary state probabilities of the MC can be obtained, which are approximately given by

$$\pi_0^N \approx \frac{1}{2}\epsilon_0 \left(\frac{1}{\Omega_1} + \frac{1}{\Omega_2}\right), \quad \pi_1^N \approx \frac{1}{2}, \tag{42}$$

$$\pi_2^N \approx \frac{1}{2}, \pi_3^N \approx \frac{1}{2}\frac{\epsilon_R}{\Omega_R}, \tag{43}$$

at high SNR. Thus, the outage probability of the NOMA scheme can be obtained as follows:

$$P_{sys}^N \approx \frac{1}{2}\left[\epsilon_0 \left(\frac{1}{\Omega_1} + \frac{1}{\Omega_2}\right) + \frac{\epsilon_R}{\Omega_R}\right]^2. \tag{44}$$

Furthermore, it is easy to prove that the diversity gain regarding to P_{sys}^N is 2.

B. FIXED POWER CONTROL

1) CASE I ($r_0 \geq 1$)

Based on the expression of $P_{\mathcal{R}_3}$ in (7) for fixed PC, we have

$$\begin{aligned} P_{\mathcal{R}_3} &= \frac{\Omega_2}{\Omega_1 + \Omega_2} e^{-\epsilon_0 2^{r_0}\left(\frac{1}{\Omega_1} + \frac{1}{\Omega_2}\right) + \frac{\epsilon_0}{\Omega_1}} \\ &\quad + \frac{\Omega_1}{\Omega_1 + \Omega_2} e^{-\epsilon_0 2^{r_0}\left(\frac{1}{\Omega_1} + \frac{1}{\Omega_2}\right) + \frac{\epsilon_0}{\Omega_2}} \\ &\approx 1 - \epsilon_0 2^{r_0}\left(\frac{1}{\Omega_1} + \frac{1}{\Omega_2}\right) + \frac{\epsilon_0\left({\Omega_1}^2 + {\Omega_2}^2\right)}{(\Omega_1 + \Omega_2)\Omega_1\Omega_2} \\ &\approx 1 - \epsilon_0 2^{r_0}\left(\frac{1}{\Omega_1} + \frac{1}{\Omega_2}\right), \end{aligned} \tag{45}$$

if $r_0 \geq 1$. In addition, each transition probability can be then approximated as

$$P_0^0 = 1 - P_{\mathcal{R}_3} \approx \epsilon_0 2^{r_0}\left(\frac{1}{\Omega_1} + \frac{1}{\Omega_2}\right), \tag{46}$$

$$P_1^1 = P_2^2 = (1 - P_{\mathcal{R}_3})(1 - P_{\mathcal{R}_4}) \approx \frac{\epsilon_0 \epsilon_R}{\Omega_R} 2^{r_0}\left(\frac{1}{\Omega_1} + \frac{1}{\Omega_2}\right), \tag{47}$$

$$P_3^3 = 1 - P_{\mathcal{R}_4} \approx \frac{\epsilon_R}{\Omega_R}, \tag{48}$$

$$P_0^1 = P_1^2 = P_{\mathcal{R}_3} \approx 1 - \epsilon_0 2^{r_0}\left(\frac{1}{\Omega_1} + \frac{1}{\Omega_2}\right), \tag{49}$$

$$P_2^3 = P_{\mathcal{R}_3}(1 - P_{\mathcal{R}_4}) \approx \frac{\epsilon_R}{\Omega_R}\left[1 - \epsilon_0 2^{r_0}\left(\frac{1}{\Omega_1} + \frac{1}{\Omega_2}\right)\right], \tag{50}$$

$$P_3^2 = P_2^1 = P_{\mathcal{R}_4} \approx 1 - \frac{\epsilon_R}{\Omega_R}, \tag{51}$$

$$P_1^0 = P_{\mathcal{R}_4}(1 - P_{\mathcal{R}_3}) \approx \left(1 - \frac{\epsilon_R}{\Omega_R}\right)\left[\epsilon_0 2^{r_0}\left(\frac{1}{\Omega_1} + \frac{1}{\Omega_2}\right)\right], \tag{52}$$

at high SNR. Based on the above transition probabilities, the stationary state probabilities of the MC can be obtained, which are approximately given by

$$\begin{aligned} \pi_0^N &\approx \frac{1}{4}\left[\left(2 - \frac{\epsilon_R}{\Omega_R}\right)\epsilon_0 2^{r_0}\left(\frac{1}{\Omega_1} + \frac{1}{\Omega_2}\right)\right] \\ &\approx \frac{1}{2}\epsilon_0 2^{r_0}\left(\frac{1}{\Omega_1} + \frac{1}{\Omega_2}\right), \end{aligned} \tag{53}$$

$$\begin{aligned} \pi_1^N &\approx \frac{1}{4}\left[2 - \epsilon_0 2^{r_0}\left(\frac{1}{\Omega_1} + \frac{1}{\Omega_2}\right)\left(1 - \frac{\epsilon_R}{\Omega_R}\right) - \frac{\epsilon_R}{\Omega_R}\right] \\ &\approx \frac{1}{2}, \end{aligned} \tag{54}$$

$$\begin{aligned} \pi_2^N &\approx \frac{1}{4}\left[2 - \epsilon_0 2^{r_0}\left(\frac{1}{\Omega_1} + \frac{1}{\Omega_2}\right)\left(1 - \frac{\epsilon_R}{\Omega_R}\right) - \frac{\epsilon_R}{\Omega_R}\right] \\ &\approx \frac{1}{2}, \end{aligned} \tag{55}$$

$$\pi_3^N \approx \frac{1}{4}\frac{\epsilon_R}{\Omega_R}\left[2 - \epsilon_0 2^{r_0}\left(\frac{1}{\Omega_1} + \frac{1}{\Omega_2}\right)\right] \approx \frac{1}{2}\frac{\epsilon_R}{\Omega_R}. \tag{56}$$

Thus, the outage probability of the NOMA scheme can be obtained as follows:

$$P_{sys}^N \approx \frac{1}{2}\left[\epsilon_0 2^{r_0}\left(\frac{1}{\Omega_1} + \frac{1}{\Omega_2}\right) + \frac{\epsilon_R}{\Omega_R}\right]^2, \tag{57}$$

and it is easy to prove that the diversity gain regarding to P_{sys}^{N} is 2.

2) CASE II ($r_0 < 1$)

Based on the expression of $P_{\mathcal{R}_3}$ in (7) for fixed PC, we further simplify $P_{\mathcal{R}_3}$ in (58) at the bottom of this page. Then, each transition probability can be approximated as

$$\begin{aligned} P_0^0 &= 1 - P_{\mathcal{R}_3} \\ &\approx \frac{\Omega_1}{\Omega_1 + \Omega_2(2^{r_0}-1)}\epsilon_0\left(\frac{1}{\Omega_1}2^{r_0} + \frac{1}{\Omega_2}\right) \\ &\quad + \frac{\Omega_2}{\Omega_1(2^{r_0}-1)+\Omega_2}\epsilon_0\left(\frac{1}{\Omega_1} + \frac{1}{\Omega_2}2^{r_0}\right) \end{aligned} \tag{59}$$

$$\begin{aligned} P_1^1 &= P_2^2 = (1-P_{\mathcal{R}_3})(1-P_{\mathcal{R}_4}) \\ &\approx \frac{\epsilon_0\epsilon_R}{\Omega_R}\left[\frac{\Omega_1}{\Omega_1 + \Omega_2(2^{r_0}-1)}\left(\frac{1}{\Omega_1}2^{r_0} + \frac{1}{\Omega_2}\right)\right. \\ &\quad \left. + \frac{\Omega_2}{\Omega_1(2^{r_0}-1)+\Omega_2}\left(\frac{1}{\Omega_1} + \frac{1}{\Omega_2}2^{r_0}\right)\right], \end{aligned} \tag{60}$$

$$P_3^3 = 1 - P_{\mathcal{R}_4} \approx \frac{\epsilon_R}{\Omega_R}, \tag{61}$$

$$\begin{aligned} P_0^1 &= P_1^2 = P_{\mathcal{R}_3} \\ &\approx 1 - \frac{\Omega_1}{\Omega_1 + \Omega_2(2^{r_0}-1)}\epsilon_0\left(\frac{1}{\Omega_1}2^{r_0} + \frac{1}{\Omega_2}\right) \\ &\quad - \frac{\Omega_2}{\Omega_1(2^{r_0}-1)+\Omega_2}\epsilon_0\left(\frac{1}{\Omega_1} + \frac{1}{\Omega_2}2^{r_0}\right), \end{aligned} \tag{62}$$

$$\begin{aligned} P_2^3 &= P_{\mathcal{R}_3}(1-P_{\mathcal{R}_4}) \\ &\approx \frac{\epsilon_R}{\Omega_R}\left[1 - \frac{\Omega_1}{\Omega_1 + \Omega_2(2^{r_0}-1)}\epsilon_0\left(\frac{1}{\Omega_1}2^{r_0} + \frac{1}{\Omega_2}\right)\right. \\ &\quad \left. - \frac{\Omega_2}{\Omega_1(2^{r_0}-1)+\Omega_2}\epsilon_0\left(\frac{1}{\Omega_1} + \frac{1}{\Omega_2}2^{r_0}\right)\right), \end{aligned} \tag{63}$$

$$P_3^2 = P_2^1 = P_{\mathcal{R}_4} \approx 1 - \frac{\epsilon_R}{\Omega_R}, \tag{64}$$

$$\begin{aligned} P_1^0 &= P_{\mathcal{R}_4}(1-P_{\mathcal{R}_3}) \\ &\approx \left(1 - \frac{\epsilon_R}{\Omega_R}\right)\left[\frac{\Omega_1}{\Omega_1 + \Omega_2(2^{r_0}-1)}\epsilon_0\left(\frac{1}{\Omega_1}2^{r_0} + \frac{1}{\Omega_2}\right)\right. \\ &\quad \left. + \frac{\Omega_2}{\Omega_1(2^{r_0}-1)+\Omega_2}\epsilon_0\left(\frac{1}{\Omega_1} + \frac{1}{\Omega_2}2^{r_0}\right)\right], \end{aligned} \tag{65}$$

at high SNR. Based on the above transition probabilities, the stationary state probabilities of the MC can be obtained, which are approximately given by

$$\begin{aligned} \pi_0^N &\approx \frac{1}{4}\left(2 - \frac{\epsilon_R}{\Omega_R}\right)\left[\frac{\Omega_1\epsilon_0}{\Omega_1 + \Omega_2(2^{r_0}-1)}\left(\frac{2^{r_0}}{\Omega_1} + \frac{1}{\Omega_2}\right)\right. \\ &\quad \left. + \frac{\Omega_2\epsilon_0}{\Omega_1(2^{r_0}-1)+\Omega_2}\left(\frac{1}{\Omega_1} + \frac{2^{r_0}}{\Omega_2}\right)\right] \\ &\approx \frac{1}{2}\left[\frac{\Omega_1\epsilon_0}{\Omega_1 + \Omega_2(2^{r_0}-1)}\left(\frac{2^{r_0}}{\Omega_1} + \frac{1}{\Omega_2}\right)\right. \\ &\quad \left. + \frac{\Omega_2\epsilon_0}{\Omega_1(2^{r_0}-1)+\Omega_2}\left(\frac{1}{\Omega_1} + \frac{2^{r_0}}{\Omega_2}\right)\right], \end{aligned} \tag{66}$$

$$\begin{aligned} \pi_1^N &\approx \frac{1}{4}\left\{2 - \left[\frac{\Omega_1\epsilon_0}{\Omega_1 + \Omega_2(2^{r_0}-1)}\left(\frac{2^{r_0}}{\Omega_1} + \frac{1}{\Omega_2}\right)\right.\right. \\ &\quad \left. + \frac{\Omega_2\epsilon_0}{\Omega_1(2^{r_0}-1)+\Omega_2}\left(\frac{1}{\Omega_1} + \frac{2^{r_0}}{\Omega_2}\right)\right] \\ &\quad \left.\times\left(1 - \frac{\epsilon_R}{\Omega_R}\right) - \frac{\epsilon_R}{\Omega_R}\right\} \approx \frac{1}{2}, \end{aligned} \tag{67}$$

$$\begin{aligned} \pi_2^N &\approx \frac{1}{4}\left\{2 - \left[\frac{\Omega_1\epsilon_0}{\Omega_1 + \Omega_2(2^{r_0}-1)}\left(\frac{2^{r_0}}{\Omega_1} + \frac{1}{\Omega_2}\right)\right.\right. \\ &\quad \left. + \frac{\Omega_2\epsilon_0}{\Omega_1(2^{r_0}-1)+\Omega_2}\left(\frac{1}{\Omega_1} + \frac{2^{r_0}}{\Omega_2}\right)\right] \\ &\quad \left.\times\left(1 - \frac{\epsilon_R}{\Omega_R}\right) - \frac{\epsilon_R}{\Omega_R}\right\} \approx \frac{1}{2}, \end{aligned} \tag{68}$$

$$\begin{aligned} \pi_3^N &\approx \frac{1}{4}\frac{\epsilon_R}{\Omega_R}\left[2 - \frac{\Omega_1\epsilon_0}{\Omega_1 + \Omega_2(2^{r_0}-1)}\left(\frac{2^{r_0}}{\Omega_1} + \frac{1}{\Omega_2}\right)\right. \\ &\quad \left. - \frac{\Omega_2\epsilon_0}{\Omega_1(2^{r_0}-1)+\Omega_2}\left(\frac{1}{\Omega_1} + \frac{2^{r_0}}{\Omega_2}\right)\right] \approx \frac{1}{2}\frac{\epsilon_R}{\Omega_R}. \end{aligned} \tag{69}$$

Thus, the outage probability of the NOMA scheme can be obtained as follows:

$$\begin{aligned} P_{sys}^N &\approx \frac{1}{2}\left[\frac{\Omega_1\epsilon_0}{\Omega_1 + \Omega_2(2^{r_0}-1)}\left(\frac{2^{r_0}}{\Omega_1} + \frac{1}{\Omega_2}\right)\right. \\ &\quad \left. + \frac{\Omega_2\epsilon_0}{\Omega_1(2^{r_0}-1)+\Omega_2}\left(\frac{1}{\Omega_1} + \frac{1}{\Omega_2 2^{r_0}}\right) + \frac{\epsilon_R}{\Omega_R}\right]^2, \end{aligned} \tag{70}$$

and the diversity gain regarding to P_{sys}^N can be proved to be 2.

On the other hand, increasing L obviously benefits to decrease the outage probability, and hence the proposed hybrid NOMA/OMA scheme achieves the diversity gain of 2 as long as $L \geq 3$, in both the scenarios of dynamic and fixed PCs at the users.

$$\begin{aligned} P_{\mathcal{R}_3} &= \frac{\Omega_1}{\Omega_1 + \Omega_2(2^{r_0}-1)}e^{-\epsilon_0\left(\frac{1}{\Omega_1}2^{r_0} + \frac{1}{\Omega_2}\right)} + \frac{\Omega_2}{\Omega_1(2^{r_0}-1)+\Omega_2}e^{-\epsilon_0\left(\frac{1}{\Omega_1} + \frac{1}{\Omega_2}2^{r_0}\right)} \\ &\quad - e^{-\left(\frac{1}{\Omega_1} + \frac{1}{\Omega_2}\right)\frac{\epsilon_0}{2-2^{r_0}}}\left[\frac{\Omega_2}{\Omega_1(2^{r_0}-1)+\Omega_2} - \frac{\Omega_2(2^{r_0}-1)}{\Omega_1 + \Omega_2(2^{r_0}-1)}\right] \\ &\approx 1 - \frac{\Omega_1}{\Omega_1 + \Omega_2(2^{r_0}-1)}\epsilon_0\left(\frac{1}{\Omega_1}2^{r_0} + \frac{1}{\Omega_2}\right) - \frac{\Omega_2}{\Omega_1(2^{r_0}-1)+\Omega_2}\epsilon_0\left(\frac{1}{\Omega_1} + \frac{1}{\Omega_2}2^{r_0}\right) \\ &\quad + \left[\frac{\Omega_2}{\Omega_1(2^{r_0}-1)+\Omega_2} - \frac{\Omega_2(2^{r_0}-1)}{\Omega_1 + \Omega_2(2^{r_0}-1)}\right]\left(\frac{1}{\Omega_1} + \frac{1}{\Omega_2}\right)\frac{\epsilon_0}{2-2^{r_0}} \\ &\approx 1 - \frac{\Omega_1}{\Omega_1 + \Omega_2(2^{r_0}-1)}\epsilon_0\left(\frac{1}{\Omega_1}2^{r_0} + \frac{1}{\Omega_2}\right) - \frac{\Omega_2}{\Omega_1(2^{r_0}-1)+\Omega_2}\epsilon_0\left(\frac{1}{\Omega_1} + \frac{1}{\Omega_2}2^{r_0}\right) \end{aligned} \tag{58}$$

ACKNOWLEDGMENT

This article was presented in part at 15th EAI International Conference on Heterogeneous Networking for Quality, Reliability, Security and Robustness, Shenzhen, China, November 2019.

REFERENCES

[1] Z. Ding, X. Lei, G. K. Karagiannidis, R. Schober, J. Yuan, and V. Bhargava, "A survey on non-orthogonal multiple access for 5G networks: Research challenges and future trends," *IEEE J. Sel. Areas Commun.*, vol. 35, no. 10, pp. 2181–2195, Oct. 2017.

[2] Z. Ding, Z. Yang, P. Fan, and H. V. Poor, "On the performance of non-orthogonal multiple access in 5G systems with randomly deployed users," *IEEE Signal Process. Lett.*, vol. 21, no. 12, pp. 1501–1505, Dec. 2014.

[3] Z. Yang, Z. Ding, P. Fan, and N. Al-Dhahir, "A general power allocation scheme to guarantee quality of service in downlink and uplink NOMA systems," *IEEE Trans. Wireless Commun.*, vol. 15, no. 11, pp. 7244–7257, Nov. 2016.

[4] P. Xu and K. Cumanan, "Optimal power allocation scheme for non-orthogonal multiple access with α-fairness," *IEEE J. Sel. Areas Commun.*, vol. 35, no. 10, pp. 2357–2369, Oct. 2017.

[5] Z. Ding, M. Peng, and H. V. Poor, "Cooperative non-orthogonal multiple access in 5G systems," *IEEE Commun. Lett.*, vol. 19, no. 8, pp. 1462–1465, Aug. 2015.

[6] J.-B. Kim and I.-H. Lee, "Non-orthogonal multiple access in coordinated direct and relay transmission," *IEEE Commun. Lett.*, vol. 19, no. 11, pp. 2037–2040, Nov. 2015.

[7] H. Liu, Z. Ding, K. J. Kim, K. S. Kwak, and H. V. Poor, "Decode-and-forward relaying for cooperative NOMA systems with direct links," *IEEE Trans. Wireless Commun.*, vol. 17, no. 12, pp. 8077–8093, Dec. 2018.

[8] Z. Yang, Z. Ding, Y. Wu, and P. Fan, "Novel relay selection strategies for cooperative NOMA," *IEEE Trans. Veh. Tech.*, vol. 66, no. 11, pp. 10114–10123, Nov. 2017.

[9] P. Xu, Z. Yang, Z. Ding, and Z. Zhang, "Optimal relay selection schemes for cooperative NOMA," *IEEE Trans. Veh. Technol.*, vol. 67, no. 8, pp. 7851–7855, Aug. 2018.

[10] M. Oiwa, C. Tosa, and S. Sugiura, "Theoretical analysis of hybrid buffer-aided cooperative protocol based on max–max and max–link relay selections," *IEEE Trans. Veh. Technol.*, vol. 65, no. 11, pp. 9236–9246, Nov. 2016.

[11] J. Zhao, Z. Ding, P. Fan, Z. Yang, and G. K. Karagiannidis, "Dual relay selection for cooperative NOMA with distributed space time coding," *IEEE Access*, vol. 6, pp. 20440–20450, 2018.

[12] M. F. Kader and S. Y. Shin, "Coordinated direct and relay transmission using uplink NOMA," *IEEE Wireless Commun. Lett.*, vol. 7, no. 3, pp. 400–403, Jun. 2018.

[13] N. Zlatanov, A. Ikhlef, T. Islam, and R. Schober, "Buffer-aided cooperative communications: Opportunities and challenges," *IEEE Commun. Mag.*, vol. 52, no. 4, pp. 146–153, Apr. 2014.

[14] N. Zlatanov, R. Schober, and P. Popovski, "Buffer-aided relaying with adaptive link selection," *IEEE J. Sel. Areas Commun.*, vol. 31, no. 8, pp. 1530–1542, Aug. 2013.

[15] V. Jamali, N. Zlatanov, and R. Schober, "Bidirectional buffer-aided relay networks with fixed rate transmission—Part II: Delay-constrained case," *IEEE Trans. Wireless Commun.*, vol. 14, no. 3, pp. 1339–1355, Mar. 2015.

[16] K. T. Pan, T. Le-Ngoc, and L. B. Le, "Optimal resource allocation for buffer-aided relaying with statistical QoS constraint," *IEEE Trans. Commun.*, vol. 64, no. 3, pp. 959–972, Mar. 2016.

[17] Z. Tian, G. Chen, Y. Gong, Z. Chen, and J. A. Chambers, "Buffer-aided max-link relay selection in amplify-and-forward cooperative networks," *IEEE Trans. Veh. Technol.*, vol. 64, no. 2, pp. 553–565, Feb. 2015.

[18] G. Chen, Z. Tian, Y. Gong, and J. Chambers, "Decode-and-forward buffer-aided relay selection in cognitive relay networks," *IEEE Trans. Veh. Technol.*, vol. 63, no. 9, pp. 4723–4728, Nov. 2014.

[19] Z. Tian, Y. Gong, G. Chen, and J. A. Chambers, "Buffer-aided relay selection with reduced packet delay in cooperative networks," *IEEE Trans. Veh. Tech.*, vol. 66, no. 3, pp. 2567–2575, Mar. 2016.

[20] I. Krikidis, T. Charalambous, and J. S. Thompson, "Buffer-aided relay selection for cooperative diversity systems without delay constraints," *IEEE Trans. Wireless Commun.*, vol. 11, no. 5, pp. 1957–1967, May 2012.

[21] N. Nomikos, T. Charalambous, I. Krikidis, D. N. Skoutas, D. Vouyioukas, and M. Johansson, "A buffer-aided successive opportunistic relay selection scheme with power adaptation and inter-relay interference cancellation for cooperative diversity systems," *IEEE Trans. Commun.*, vol. 63, no. 5, pp. 1623–1634, May 2015.

[22] P. Xu, Z. Ding, I. Krikidis, and X. Dai, "Achieving optimal diversity gain in buffer-aided relay networks with small buffer size," *IEEE Trans. Veh. Technol.*, vol. 65, no. 10, pp. 8788–8794, Oct. 2016.

[23] S. Luo and K. C. Teh, "Adaptive transmission for cooperative NOMA system with buffer-aided relaying," *IEEE Commun. Lett.*, vol. 21, no. 4, pp. 937–940, Apr. 2017.

[24] Q. Zhang, Z. Liang, Q. Li, and J. Qin, "Buffer-aided non-orthogonal multiple access relaying systems in Rayleigh fading channels," *IEEE Trans. Commun.*, vol. 65, no. 1, pp. 95–106, Jan. 2017.

[25] N. Nomikos, T. Charalambous, D. Vouyioukas, G. K. Karagiannidis, and R. Wichman, "Relay selection for buffer-aided non-orthogonal multiple access networks," in *Proc. IEEE Globecom Workshops*, Singapore, Dec. 2017, pp. 1–6.

[26] T. M. C. Chu and H.-J. Zepernick, "Performance of a non-orthogonal multiple access system with full-duplex relaying," *IEEE Commun. Lett.*, vol. 22, no. 10, pp. 2084–2087, Oct. 2018.

[27] N. Nomikos, T. Charalambous, D. Vouyioukas, G. K. Karagiannidis, and R. Wichman, "Hybrid NOMA/OMA with buffer-aided relay selection in cooperative networks," *IEEE J. Sel. Topics Signal Process.*, vol. 13, no. 3, pp. 524–537, Jun. 2019.

[28] M. Alkhawatrah, Y. Gong, G. Chen, S. Lambotharan, and J. A. Chambers, "Buffer-aided relay selection for cooperative NOMA in the Internet of Things," *IEEE Internet Things J.*, vol. 6, no. 3, pp. 5722–5731, Jun. 2019.

[29] T. M. Cover and J. A. Thomas, *Elements of Information Theory*, 2nd ed. New York, NY, USA: Wiley, 2006.

[30] Z. Ning, J. Huang, X. Wang, J. J. P. C. Rodrigues, and L. Guo, "Mobile edge computing-enabled Internet of Vehicles: Toward energy-efficient scheduling," *IEEE Netw.*, vol. 33, no. 5, pp. 198–205, Sep./Oct. 2019.

[31] Z. Zhang, C. Wang, C. Gan, S. Sun, and M. Wang, "Automatic modulation classification using convolutional neural network with features fusion of SPWVD and BJD," *IEEE Trans. Signal Inf. Process. Netw.*, vol. 5, no. 3, pp. 469–478, Sep. 2019.

[32] Z. Ning, Y. Feng, M. Collotta, X. Kong, X. Wang, and L. Guo, "Deep learning in edge of vehicles: Exploring trirelationship for data transmission," *IEEE Trans. Ind. Informat.*, vol. 15, no. 10, pp. 5737–5746, Oct. 2019.

[33] Z. Ning, P. Dong, X. Wang, M. S. Obaidat, X. Hu, L. Guo, Y. Guo, J. Huang, B. Hu, and Y. Li, "When deep reinforcement learning meets 5G vehicular networks: A distributed offloading framework for traffic big data," *IEEE Trans. Ind. Informat.*, to be published.

[34] S. Luo and K. C. Teh, "Buffer state based relay selection for buffer-aided cooperative relaying systems," *IEEE Trans. Wireless Commun.*, vol. 14, no. 10, pp. 5430–5439, Oct. 2015.

[35] J. R. Norris, *Markov Chain*. Cambridge, U.K.: Cambridge Univ. Press, 1997.

PENG XU (M'17) received the B.Eng. and Ph.D. degrees in electronic and information engineering from the University of Science and Technology of China, Hefei, Anhui, China, in 2009 and 2014, respectively. Since July 2014, he has been a Postdoctoral Researcher with the Department of Electronic Engineering and Information Science, University of Science and Technology of China. He is currently an Associate Professor with the School of Communication and Information Engineering, Chongqing University of Posts and Telecommunications, China. His current research interests include cooperative communications, information theory, information-theoretic secrecy, and 5G networks. He received the IEEE Wireless Communications Letters Exemplary Reviewer 2015.

JIANPING QUAN received the B.S. degree in communication engineering from the Chongqing University of Posts and Telecommunications, Chongqing, China, in 2019, where she is currently pursuing the M.S. degree. Her research interests include non-orthogonal multiple access, cooperative communication, and buffer-aided relaying.

ZHENG YANG (S'12–M'16) received the B.S. degree in mathematics from Minnan Normal University, Zhangzhou, in 2008, the M.S. degree in mathematics from Fujian Normal University, Fuzhou, China, in 2011, and the Ph.D. degree in information and communications engineering from Southwest Jiaotong University, Chengdu, China, in 2016. He was a Visiting Ph.D. Student with the School of Electrical and Electronic Engineering, Newcastle University, Newcastle upon Tyne, U.K., in 2014. He is currently an Associate Professor with the College of Photonic and Electronic Engineering, Fujian Normal University. His research interests include 5G networks, cooperative and energy harvesting networks, and signal design and coding. He received the Excellent Doctoral Thesis Award from the China Education Society of Electronics, in 2017, and the 2018 IEEE Signal Processing Society Best Signal Processing Letter Award.

GAOJIE CHEN (S'09–M'12–SM'18) received the B.Eng. and B.Ec. degrees in electrical information engineering and international economics and trade from Northwest University, China, in 2006, and the M.Sc. (Hons.) and Ph.D. degrees in electrical and electronic engineering from Loughborough University, Loughborough, U.K., in 2008 and 2012, respectively. From 2008 to 2009, he was a Software Engineering with DTmobile, Beijing, China, and from 2012 to 2013, he was a Research Associate with the School of Electronic, Electrical and Systems Engineering, Loughborough University. He was a Research Fellow with 5GIC, Faculty of Engineering and Physical Sciences, University of Surrey, U.K., from 2014 to 2015. He was a Research Associate with the Department of Engineering Science, University of Oxford, U.K., from 2015 to 2018. He is currently a Lecturer with the Department of Engineering, University of Leicester, U.K. His research interests include information theory, wireless communications, the IoT, cognitive radio, secrecy communication, and random geometric networks. He received the Exemplary Reviewer Certificate of the IEEE Wireless Communication Letters, in 2018. He currently serves as an Editor of the *IET Electronics Letters*.

ZHIGUO DING (S'03–M'05) received the B.Eng. degree in electrical engineering from the Beijing University of Posts and Telecommunications, in 2000, and the Ph.D. degree in electrical engineering from Imperial College London, in 2005. From July 2005 to April 2018, he was working in Queen's University Belfast, Imperial College, Newcastle University, and Lancaster University. Since April 2018, he has been with The University of Manchester as a Professor in communications. From October 2012 to September 2020, he has also been an Academic Visitor with Princeton University. His research interests include 5G networks, game theory, cooperative and energy harvesting networks, and statistical signal processing.

Dr. Ding received the Best Paper Award in the IET ICWMC-2009 and the IEEE WCSP-2014, the EU Marie Curie Fellowship 2012–2014, the Top IEEE TVT Editor 2017, the IEEE Heinrich Hertz Award 2018, the IEEE Jack Neubauer Memorial Award 2018, and the IEEE Best Signal Processing Letter Award 2018. He was an Editor for the IEEE Wireless Communication Letters and the IEEE Communication Letters, from 2013 to 2016. He is serving as an Area Editor for the IEEE Open Journal of the Communications Society and an Editor for the IEEE Transactions on Communications, the IEEE Transactions on Vehicular Technology, and *Journal of Wireless Communications and Mobile Computing*.